DEVELOPMENT OF

SENSITIVITY ANALYSIS AND OPTIMIZATION

FOR MICROWAVE CIRCUITS AND ANTENNAS IN

THE FREQUENCY DOMAIN

DEVELOPMENT OF SENSITIVITY ANALYSIS AND OPTIMIZATION FOR MICROWAVE CIRCUITS AND ANTENNAS IN THE FREQUENCY DOMAIN

By

Jiang Zhu, B. Sc. (Eng.)

A Thesis

Submitted to the School of Graduate Studies

in Partial Fulfillment of the Requirements

for the Degree

Master of Applied Science

McMaster University

MASTER OF APPLIED SCIENCE (2006) McMASTER UNIVERSITY
(Electrical and Computer Engineering) Hamilton, Ontario

TITLE: **Development of Sensitivity Analysis and Optimization for Microwave Circuits and Antennas in the Frequency Domain**

AUTHOR: Jiang Zhu
B.Sc. (Eng) (Electrical Engineering, Zhejiang University)

SUPERVISORS: Natalia Nikolova, Associate Professor,
Department of Electrical and Computer Engineering
Dipl.Eng. (Technical University of Varna)
Ph.D. (University of Electro-Communication)
P.Eng. (Province of Ontario)
Senior Member, IEEE

J.W. Bandler, Professor Emeritus,
Department of Electrical and Computer Engineering
B.Sc.(Eng), Ph.D., D.Sc.(Eng) (University of London)
D.I.C. (Imperial College)
P.Eng. (Province of Ontario)
C.Eng., FIEE (United Kingdom)
Fellow, IEEE
Fellow, Royal Society of Canada
Fellow, Engineering Institute of Canada
Fellow, Canadian Academy of Engineering

NUMBER OF PAGES: xviii, 137

ABSTRACT

This thesis contributes to the development of adjoint variable methods (AVM) and space mapping (SM) technology for computer-aided electromagnetics (EM)-based modeling and design of microwave circuits and antennas.

The AVM is known as an efficient approach to design sensitivity analysis for problems of high complexity. We propose a general self-adjoint approach to the sensitivity analysis of network parameters for an Method of Moments (MoM) solver. It requires neither an adjoint problem nor analytical system matrix derivatives. For the first time, we suggest practical and fast sensitivity solutions realized entirely outside the EM solver, which simplifies the implementation. We discuss: (1) features of commercial EM solvers which allow the user to compute network parameters and their sensitivities through a single full-wave simulation; (2) the accuracy of the computed derivatives; (3) the overhead of the sensitivity computation. Our approach is demonstrated by FEKO, which employs an MoM solver.

One motivation for sensitivity analysis is gradient-based optimization. The sensitivity evaluation providing the Jacobian is a bottleneck of optimization with full-wave simulators. We propose an approach, which employs the self-adjoint

sensitivity analysis of network parameters and Broyden's update for practical EM design optimization. The Broyden's update is carried out at the system matrix level, so that the computational overhead of the Jacobian is negligible while the accuracy is acceptable for optimization. To improve the robustness of the Broyden update in the sensitivity analysis, we propose a switching criterion between the Broyden and the finite-difference estimation of the system matrix derivatives.

In the second part, we apply for the first time a space mapping technique to antenna design. We exploit a coarse mesh MoM solver as the coarse model and align it with the fine mesh MoM solution through space mapping. Two SM plans are employed: I. implicit SM and output SM, and II. input SM and output SM. A novel local meshing method is proposed to avoid inconsistencies in the coarse model. The proposed techniques are implemented through the new user-friendly SMF system. In a double annular ring antenna example, the *S*-parameter is optimized. The finite ground size effect for the MoM is efficiently solved by SM Plan I and the design specification is satisfied after only three iterations. In a patch antenna example, we optimize the impedance through both plans. Comparisons are made. Coarseness in the coarse model and its effect on the SM performance is also discussed.

ACKNOWLEDGEMENTS

The author wishes to express his sincere appreciation to his supervisors Dr. Natalia K. Nikolova and Dr. John. W. Bandler, the Computational Electromagnetics Laboratory and the Simulation Optimization Systems Research Laboratory, McMaster University, for their expert supervision, continuing encouragement and constant support during the course of this work.

The author would like to express his appreciation to Dr. Mohamed H. Bakr, Dr. Slawomir Koziel, Dr. Ahmed S. Mohamed, Dr. Qingsha Cheng, Mr. Dongying Li and Mr. Wenhuan Yu, his colleagues from the Computational Electromagnetics Laboratory and the Simulation Optimization Systems Research Laboratory of the Department of Electrical and Computer Engineering at McMaster University, for useful collaboration and stimulating discussions.

The author wishes to acknowledge Dr. C. J. Reddy, Dr. Rensheng Sun, from EM Software & System (USA), Inc., for making the FEKO system available and for useful discussions.

The author gratefully acknowledges the financial assistance provided by the Natural Sciences and Engineering Research Council of Canada under Grants OGP0007239 and STGP269760, by Bandler Corporation and by the Department

of Electrical and Computer Engineering, McMaster University, through a Research Assistantship.

Finally, special thanks go to my family for encouragement, understanding and continuous support.

CONTENTS

LIST OF FIGURES

LIST OF FIGURES

LIST OF TABLES

LIST OF TABLES

LIST OF ACRONYMS

B-SASA	Broyden-update Self-adjoint Sensitivity Analysis
BLC	Boundary-layer Concept
CAD	Computer-Aided Design
CEM	Computational Electromagnetics
EFIE	Electric Field Integral Equation
EM	Electromagnetics
FAST	Feasible Adjoint Sensitivity Technique
FD-SASA	Finite-difference Self-adjoint Sensitivity Analysis
FDTD	Finite Difference Time Domain
FEM	Finite Element Method
GUI	Graphical User Interface
HFSS	High Frequency Structure Simulator
HTS	High-Temperature Superconductor
ISM	Implicit Space Mapping
MFIE	Magnetic Field Integral Equation
MLFMM	Multilevel Fast Multipole Method

LIST OF ACRONYM

MoM	Method of Moments
OSM	Output Space Mapping
PCB	Printed Circuit Board
PE	Parameter Extraction
PMCHW	Poggio, Miller, Chang, Harrington, Wu
RF	Radio Frequency
SASA	Self-adjoint Sensitivity Analysis
SEP	Surface Equivalent Principle
SM	Space Mapping
SMF	Space Mapping Framework
SQP	Sequential Quadratic Programming
TLM	Transmission-Line Matrix (Modeling)
TR	Trust Regions

CHAPTER 1

INTRODUCTION

1.1 MOTIVATION

The computer-aided engineering for high-frequency structures (microwave and millimeter-wave circuits and antennas) originated in the early 1950s with the advent of first-generation computers. Since then, the design and modeling of microwave circuits applying optimization techniques have been extensively researched [1]-[3].

As computing resources became more powerful and widely available, the computational electromagnetics (CEM) emerged and spurred a variety of numerical algorithms for full-wave EM analysis, including the method of moments (MoM), the finite element method (FEM), the finite difference-time domain method (FDTD), the transmission line method (TLM), etc. They solve Maxwell's equations for structures of arbitrary geometrical shapes and offer superior accuracy and complete field representation—as long as the theoretical model includes all EM field interactions. Ansoft HFSS [4], ADS Momentum [5],

Sonnet ***em*** [6], XFDTD [7], FEKO [8] and MEFiSTo-3D [9] are some common commercial full-wave analysis solvers.

However, these algorithms are extremely demanding in terms of computer memory and time. Even today, full-wave analysis appears prohibitively slow for the purposes of modeling and design of a complete microwave circuit. The problem of efficient sensitivity estimation and optimization with full-wave EM analysis remains a challenge [10].

1.2 OUTLINE OF THESIS

In this thesis, we approach solving this problem from two sides:

1) Self-adjoint sensitivity analysis (SASA) method for fast sensitivity computation and its application to EM optimization;
2) The space mapping (SM) technique for microwave circuit optimization.

We first review some relevant concepts from the method of moments [11]-[13], which is the primary numerical analysis method throughout this research. We formulate a general self-adjoint approach to the sensitivity analysis of network parameters, which requires neither an adjoint problem nor analytical system matrix derivatives [14]-[16]. Then, we propose an approach for EM design optimization, which employs the self-adjoint sensitivity analysis of network parameters and Broyden's update [17]. After that, we apply the SM techniques to antenna design. A practical SM design framework is formalized, especially

suitable for antennas as well as planar microwave circuit design [18][19]. We conclude by suggesting a combined application of the SM technique and the SASA method. This thesis is grouped into two parts.

Chapters 3 to 4 in Part I describe the self-adjoint sensitivity analysis (SASA) method and its application to EM design optimization.

Chapter 3 presents the self-adjoint formulas for network-parameter sensitivity calculation in the MoM. It requires neither an adjoint problem nor analytical system matrix derivatives. The derivative of the system matrix is obtained by the finite-difference method, so this approach is also referred to as the FD-SASA. We outline the features of the commercial EM solvers, which enable independent network-parameter sensitivity analysis. We implement our technique in FEKO, which employs MoM. Numerical examples, the patch antenna and the microstrip bandstop filter, demonstrate our approach, followed by a discussion of the MoM matrix symmetry versus convergence of the solution. Then, the computational overhead associated with the sensitivity analysis is discussed and recommendations are given for further reduction of the computational cost whenever software changes are possible.

In Chapter 4, we study EM optimization using sensitivity analysis in the frequency domain. We investigate the feasibility of the Broyden update in the computation of the system matrix derivatives [20][21] for use with our self-adjoint formula during optimization. We refer to this approach as the Broyden-update self-adjoint sensitivity analysis (B-SASA). It is applicable to sensitivity

analysis for optimization purposes due to the iterative nature of Broyden's formula. This improvement is significant compared with the FD-SASA which is proposed in Chapter 3. The B-SASA method may offer inaccurate gradient information under certain conditions. We develop a set of criteria for switching back and forth throughout the optimization process between the robust but more time-demanding FD-SASA and the B-SASA. This hybrid approach (B/FD-SASA) guarantees good accuracy of gradient information with minimal computational time.

Chapter 5 in Part II presents the antenna design optimization exploiting SM techniques.

In Chapter 5, we apply space mapping technique (see [1]-[3], [22]-[25]) to antenna design. We exploit a coarse-mesh MoM solver as the coarse model and align it with the fine-mesh MoM solution through SM. We employ two space mapping plans. The first plan includes implicit SM and output SM. The second plan includes input SM and output SM. A novel local meshing method avoids inconsistencies in the coarse model. The proposed techniques are implemented through the SMF (Space Mapping Framework) system. In a double annular ring antenna example, the *S*-parameter is optimized. The finite ground size effect for the MoM is effectively solved by space mapping plan I and the design specification is satisfied after only three iterations. In a patch antenna example, we optimize the impedance with both plans. Comparisons are made. Coarseness

in the coarse model and its effect on the space mapping performance are discussed.

The thesis is concluded with suggestions for further research. For convenience, a bibliography is given at the end of thesis.

1.3 CONTRIBUTIONS

The author contributed substantially to the following original developments presented in this thesis:

I. Development of a self-adjoint sensitivity analysis algorithm for the method of moments.

II. Implementation of the self-adjoint sensitivity analysis algorithm with the commercial EM software FEKO.

III. Development of a mixed self-adjoint sensitivity analysis algorithm (B/FD-SASA) for frequency domain EM optimization using sensitivity analysis.

IV. Development and implementation of a CAD algorithm for antenna design utilizing space mapping.

V. Development of a coarse-mesh surrogate model optimization algorithm for the method of moments.

VI. Contribution to developing the FEKO driver of the SMF system which automatically executes FEKO, updates parameters and extracts responses in Mablab.

REFERENCES

[1] A.S. Mohamed, *Recent Trends in CAD Tools for Microwave Circuit Design Exploiting Space Mapping Technology*, PhD Thesis, Department of Electrical and Computer Engineering, McMaster University, 2005.

[2] Q. Cheng, *Advances in Space Mapping Technology Exploiting Implicit Space Mapping and Output Space Mapping*, PhD Thesis, Department of Electrical and Computer Engineering, McMaster University, 2004.

[3] M.H. Bakr, *Advances in Space Mapping Optimization of Microwave Circuits*, PhD Thesis, Department of Electrical and Computer Engineering, McMaster University, 2000.

[4] Ansoft HFSS, Ansoft Corporation, 225 West Station Square Drive, Suite 200, Pittsburgh, PA 15219, USA.

[5] Agilent ADS, Agilent Technologies, 1400 Fountaingrove Parkway, Santa Rosa, CA 95403-1799, USA.

[6] ***em***, Sonnet Software, Inc. 100 Elwood Davis Road, North Syracuse, NY 13212, USA.

[7] XFDTD, Remcom Inc., 315 South Allen Street, Suite 222, State College, PA 16801, USA.

[8] FEKO, Suite 4.2, June 2004, EM Software & Systems-S.A. (Pty) Ltd, 32 Techno lane, Technopark, Stellenbosch, 7600, South Africa.

[9] MEFiSTo-3D*,* Faustus Scientific Corporation, 1256 Beach Drive, Victoria, BC, V8S 2N3, Canada.

[10] N.K. Nikolova, J.W. Bandler and M.H. Bakr, "Adjoint techniques for sensitivity analysis in high-frequency structure CAD," *IEEE Trans. Microwave Theory Tech*., vol. 52, Jan. 2004, pp. 403-419.

[11] D.G. Swanson, Jr. and W.J.R. Hoefer, *Microwave Circuit Modeling Using Electromagnetic Filed Simulation*, Artech House, 2003.

[12] I.D. Robertson and S. Lucyszyn, *RFIC and MMIC design and technology*, *IEE Circuits, Device and System*, Series 13, 2001.

[13] L. Daniel, *Simulation and Modeling Techniques for Signal Integrity and Electromagnetic Interference on High Frequency Electronic Systems*, PhD Thesis, Electrical Engineering and Computer Science, University of California at Berkeley.

[14] N.K. Nikolova, J. Zhu, D. Li, M.H. Bakr and J.W. Bandler, "Sensitivity analysis of network parameters with electromagnetic frequency-domain simulators," *IEEE Trans. Microwave Theory Tech*., vol. 54, Feb. 2006, pp. 670-681.

[15] N.K. Nikolova, J. Zhu, D. Li and M.H. Bakr, "Extracting the derivatives of network parameters from frequency-domain electromagnetic solutions," the *XXVIIIth General Assembly of the International Union of Radio Science*, CDROM, Oct. 2005.

[16] J. Zhu, N.K. Nikolova and J. W. Bandler, "Self-adjoint sensitivity analysis of high-frequency structures with FEKO," the *22nd International Review of Progress in Applied Computational Electromagnetics Society* (*ACES 2006*), Miami, Florida, pp. 877-880.

[17] D. Li, J. Zhu, N.K. Nikolova, M.H. Bakr and J.W. Bandler, "EM optimization using sensitivity analysis in the frequency domain," submitted to *IEEE Trans. Antennas Propagat., Special Issue on Synthesis and Optimization Techniques in Electromagnetics and Antenna System Design*, Jan. 2007.

[18] J. Zhu, J.W. Bandler, N.K. Nikolova and S. Koziel, "Antenna optimization through space mapping," submitted to *IEEE Trans. Antennas Propagat., Special Issue on Synthesis and Optimization Techniques in Electromagnetics and Antenna System Design*, Jan. 2007.

[19] J. Zhu, J.W. Bandler, N.K. Nikolova and S. Koziel, "Antenna design through space mapping optimization," *IEEE MTT-S Int. Microwave Symp*., San Francisco, California, 2006.

[20] N.K Nikolova, R. Safian, E.A. Soliman, M.H. Bakr and J.W. Bandler, "Accelerated gradient based optimization using adjoint sensitivities," *IEEE Trans. Antenna Propagat.* vol. 52, Aug. 2004, pp. 2147-2157.

[21] J.W. Bandler, S.H. Chen, S. Daijavad and K. Madsen, "Efficient optimization with integrated gradient approximations," *IEEE Trans. Microwave Theory Tech*., vol. 36, Feb. 1988, pp. 444-455.

[22] J.W. Bandler, Q.S. Cheng, S.A. Dakroury, A.S. Mohamed, M.H. Bakr, K. Madsen and J. Søndergaard, "Trends in space mapping technology for engineering optimization," *3rd Annual McMaster Optimization Conference: Theory and Applications, MOPTA03*, Hamilton, ON, Aug. 2003.

[23] J.W. Bandler, Q. Cheng, S.A. Dakroury, A.S. Mohamed, M.H. Bakr, K. Madsen and J. Søndergaard, "Space mapping: the state of the art," in *SBMO MTT-S International Microwave and Optoelectronics Conference* (*IMOC 2003*), Parana, Brazil, Sep. 2003, vol. 2, pp. 951-956.

[24] J.W. Bandler, Q. Cheng, S.A. Dakroury, A.S. Mohamed, M.H. Bakr, K. Madsen and J. Søndergaard, "Space mapping: the state of the art," *IEEE Trans. Microwave Theory and Tech.,* vol. 52, Jan. 2004, pp. 337-361.

[25] J.W. Bandler, Q.S. Cheng, D.M. Hailu, A.S. Mohamed, M.H. Bakr, K. Madsen and F. Pedersen, "Recent trends in space mapping technology," in *Proc. 2004 Asia-Pacific Microwave Conf. APMC04* New Delhi, India, Dec. 2004.

CHAPTER 1 INTRODUCTION

CHAPTER 2

SOME RELEVANT FEATURES OF THE METHOD OF MOMENTS

2.1 BRIEF INTRODUCTION TO THE METHOD OF MOMENTS

The need for full-wave EM solvers is obvious. The major advantage of numerical techniques is that they can be applied to a structure of arbitrary shape and provide excellent accuracy.

The method of moments (MoM) is probably the most popular full-wave approach to the analysis of planar structures. Many of the well known commercial software packages exploit this method. Some notable packages are Agilent Momentum from Agilent Technologies [1], Sonnet ***em*** from Sonnet Software Inc. [2], Ansoft Ensemble from Ansoft Corporation [3], and FEKO from EMSS [4]. The method of moments is the primary numerical method used in this research on the self-adjoint sensitivity analysis [5]-[8] and space mapping for antenna optimization [9][10].

CHAPTER 2 SOME RELEVANT FEATURES OF THE METHOD OF MOMENTS

The method of moments was created to numerically solve systems of integral-differential equations. The simplest MoM employs pulse expansion functions and Dirac testing function (collocation). Harrington [11] has extended this concept by describing it in terms such that it is essentially identical to the general method of projective approximation, including collocation as a special case [12][13].

In a narrower sense, MoM is the method of choice for solving problems stated in the form of an electric field integral equation (EFIE) or a magnetic field integral equation (MFIE):

$$\text{EFIE}: \quad L_e^{-1}\boldsymbol{J} = \boldsymbol{E} \tag{2.1}$$

$$\text{MFIE}: \quad L_m^{-1}\boldsymbol{J} = \boldsymbol{H} \tag{2.2}$$

$\boldsymbol{E}$ and $\boldsymbol{H}$ are the field vectors, and $\boldsymbol{J}$ is the source function (current density). In most of the cases, these integral equations are formulated in the frequency domain although time domain applications exist. Instead of the fields $\boldsymbol{E}$ and $\boldsymbol{H}$, we may also formulate the problem in terms of scalar and vector potentials.

In the above sense, the MoM is an integral equation method for the frequency-domain analysis. Table 2.1 and Table 2.2 give the basic features of the integral methods versus the differential-methods and the frequency-domain methods versus the time domain methods, respectively [14].

In the MoM, only the surfaces of the objects are discretized. The linear system resulting from the discretization is much smaller compared to the FDTD and the FEM system matrices. The system is unfortunately very dense, because

every surface element interacts with every other surface element. This method is ideal for open field environment simulations and can handle very efficiently antenna application.

2.2 CPU TIME COST VERSUS MESH DENSITY [15]

The CPU time for a MoM simulation can be expressed as

$$\text{CPU time} = A + BN + CN^2 + DN^3 \tag{2.2}$$

where N is the number of unknowns. A, B, C and D are constants independent of N. A accounts for the simulation set-up time. The meshing of the structure leads to the linear term BN. The filling of the system matrix is responsible for the quadratic term, and solving the matrix equation for the cubic term. The values of A, B, C and D depend on the problem at hand.

The quadratic and cubic terms dominate. For small to medium size problems, as the constant C is much larger than D, the solution time is dominated by the matrix fill. For large scale problems, the matrix solving time with its cubic term will eventually dominate the CPU-time cost. Thus, for medium to large scale problems, the time saving by using coarse-mesh coarse models will be significant.

TABLE 2.1

DIFFERENTIAL EQUATION METHODS VS.

INTEGRAL EQUATION METHODS [14]

Differential Methods	Integral Methods
discretize entire domain	discretize only active region
lead to huge but sparse linear systems	lead to relatively small but dense linear systems
good for inhomogeneous materials	problems with inhomogeneous materials; good for layered materials
problems with open boundary conditions	good for open boundary conditions

TABLE 2.2

TIME DOMAIN VS FREQUENCY DOMAIN [14]

Time Domain Methods	Frequency Domain Methods
can handle non-linearities	problems with non-linearities
run a long simulation exciting all significant modes and then take a Fourier Transform.	solve for specific frequency points
can produce insightful animations	can exploit new techniques for fast calculation of the dominant eigenvalues

2.3 MESH REFINEMENT [16]

The accuracy of any simulation is dependent on the quality of the approximations being made. In the method of moments, the surface currents are approximated by a set of currents over a number of surface triangles.

Frequency domain models (including the finite element method and the method of moments) should be checked for mesh convergence. This is done by varying the size of the mesh element from one simulation to the next, and keeping all other model parameters the same. The results of these two simulations can then be compared. If there is a significant difference in the results, the surfaces are not adequately discretized and a finer mesh is needed.

The most common way to do a mesh convergence test is to reduce the global size of the mesh element. However, global refinement results in additional resource requirement throughout the model. This is a very safe way of checking convergence, but experienced users will be able to make a very good guess about where refinement might be necessary. In these cases, it would be far more efficient to refine the mesh locally, rather than globally.

2.4 MODELING OF DIELECTRIC MATERIALS [17][18]

Today's EM problems are very complex in general. It is vital to take into account the effects of lossy dielectric and magnetic materials into account, such as antenna radomes, dielectric substrates, biological tissue, etc. The traditional Special Green's Functions technique, which only models the metallic surface,

cannot fulfill such requirements. Techniques based on the volume or surface equivalent principles within the MoM aim at solving such problems.

I. The Special Green's Function technique.

A Green's function describes the response in space to a point excitation or source. The simplest form of a Green's function is the free space Green's function. It is possible to use a Special Green's Function to incorporate features of the propagation space into the model. Only the surface of metallic meshes has to be modeled. This means that the properties of the remainder of the structure are modeled implicitly, which is very computer resource efficient but is limited to a few special cases, such as the layered dielectrics.

II. The Surface Equivalent Principle (SEP) technique.

The MoM for metallic structures solves for the electric currents on the surface of all metallic objects in order to determine the electromagnetic observables, e.g., current densities at the port. When using the SEP, the surfaces of a dielectric are discretised for both the electric and the magnetic currents on the surface. All sides of a dielectric have to be modeled, making a closed solid. This means that there are now two basis functions for each triangle pair which correlates to a memory requirement of four times what it would be if the same structure was metallic.

One can imagine that for a planar structure with a finite ground, the Special Green's Function technique provides an efficient but less accurate solution, since an infinite ground plane is assumed. In contrast, since the SEP

model takes the finite ground effects into account by modeling all metallic and dielectric surfaces, its solution is accurate but more time-consuming.

In the double annular ring antenna example in Section 5.5.1, we use the Special Green's Function as the coarse model and the SEP as the fine model. Then we optimize its *S*-parameter in an efficient way by exploiting the space mapping technique.

REFERENCES

[1] Agilent ADS, Agilent Technologies, 1400 Fountaingrove Parkway, Santa Rosa, CA 95403-1799, USA.

[2] ***em***, Sonnet Software, Inc., 100 Elwood Davis Road, North Syracuse, NY 13212, USA.

[3] Ansoft Ensemble, Ansoft Corporation, 225 West Station Square Drive, Suite 200, Pittsburgh, PA 15219, USA.

[4] FEKO, Suite 4.2, June 2004, EM Software & Systems-S.A. (Pty) Ltd, 32 Techno lane, Technopark, Stellenbosch, 7600, South Africa.

[5] N.K. Nikolova, J. Zhu, D. Li, M.H. Bakr and J.W. Bandler, "Sensitivity analysis of network parameters with electromagnetic frequency-domain simulators," *IEEE Trans. Microwave Theory Tech*., vol. 54, Feb. 2006, pp. 670-681.

[6] N.K. Nikolova, J. Zhu, D. Li and M.H. Bakr, "Extracting the derivatives of network parameters from frequency-domain electromagnetic solutions," the *XXVIIIth General Assembly of the International Union of Radio Science*, Oct. 2005.

[7] J. Zhu, N.K. Nikolova and J. W. Bandler, "Self-adjoint sensitivity analysis of high-frequency structures with FEKO," the *22nd International Review of Progress in Applied Computational Electromagnetics Society* (*ACES 2006*), Miami, Florida, pp. 877-880.

[8] D. Li, J. Zhu, N.K. Nikolova, M.H. Bakr and J.W. Bandler, "EM optimization using sensitivity analysis in the frequency domain," submitted to *IEEE Trans. Antennas Propagat., Special Issue on Synthesis and Optimization Techniques in Electromagnetics and Antenna System Design*, Jan. 2007.

[9] J. Zhu, J.W. Bandler, N.K. Nikolova and S. Koziel, "Antenna optimization through space mapping," submitted to *IEEE Trans. Antennas Propagat., Special Issue on Synthesis and Optimization Techniques in Electromagnetics and Antenna System Design*, Jan. 2007.

[10] J. Zhu, J. W. Bandler, N. K. Nikolova and S. Koziel, "Antenna design through space mapping optimization," *IEEE MTT-S Int. Microwave Symp.*, San Francisco, California, 2006.

[11] R.F. Harrington, *Field Computation by Moment Methods*, New York, NY: Macmillan, 1968.

[12] D.G. Swanson, Jr. and W.J.R. Hoefer, *Microwave Circuit Modeling Using Electromagnetic Field Simulation*, Artech House, Boston. London, 2003.

[13] C.A. Balanis, *Antenna Theory: Analysis and Design*, New York: Wiley, 1997.

[14] L. Daniel, *Simulation and Modeling Techniques for Signal Integrity and Electromagnetic Interference on High Frequency Electronic Systems*, PhD Thesis, Electrical Engineering and Computer Science, University of California at Berkeley.

[15] Advanced Design System 2003C, *User's Manual*, Agilent Technologies, 395 Page Mill Road, Palo Alto, CA 94304, USA.

[16] "Mesh refinement," *FEKO Quarterly*, December 2004.

[17] "Modelling of dielectric materials in FEKO," *FEKO Quarterly*, Mar. 2005.

[18] U. Jakobus, "Comparison of different techniques for the treatment of lossy dielectric/magnetic bodies within the method of moments formulation," *AEÜ International Journal of Electronics and Communications*, vol. 54, 2000, pp. 163-173.

CHAPTER 2 SOME RELEVANT FEATURES OF THE METHOD OF MOMENTS

PART I

SENSITIVITY ANALYSIS IN THE FREQUENCY DOMAIN

CHAPTER 3

SELF-ADJOINT SENSITIVITY ANALYSIS IN THE METHOD OF MOMENTS

3.1 INTRODUCTION

The goal of frequency domain sensitivity analysis is to evaluate the gradient of the response of a system to variations of its design parameters [1]. In high-frequency structure analysis, the design parameters typically describe the structure's geometry and the electromagnetic properties of the media involved.

The computation of the gradient is often carried out using finite differences where the structure is analyzed an additional time for each independent variable. It should be obvious that this approach is viable only when the requirements of an analysis in terms of CPU times and computer memory are reasonably small [2].

The adjoint-variable method is known to be the most efficient approach to design sensitivity analysis for problems of high complexity where the number of

state variables is much greater than the number of the required response derivatives [3]-[5]. General adjoint-based methodologies have been available for some time in control theory [3], and techniques complementary to the finite-element method (FEM) have been developed in structural [4],[5] and electrical [6]-[11] engineering. However, feasible implementations remain a challenge. The reason lies mainly in the complexity of these techniques.

Recently, a simpler and more versatile approach has been adopted [1] [12]-[13] for analyses with the MoM and the frequency-domain transmission-line method. The effort to formulate analytically the system matrix derivative—which is an essential component of the sensitivity formula—was abandoned as impractical for a general-purpose sensitivity solver. Instead, approximations of the system-matrix derivatives are employed using either finite differences [1] or discrete step-wise changes [12], [13] as dictated by the nature of the discretization grid. Neither the accuracy nor the computational speed is sacrificed.

All of the above approaches require the analysis of an adjoint problem whose excitation is response dependent. Not only does this mean one additional full-wave simulation but it also requires modification of the EM analysis engine due to the specifics of the adjoint-problem excitation. Notably, Akel *et al*. [8] has pointed out that in the case of the FEM with tetrahedral edge elements, the sensitivity of the *S*-matrix can be derived without an adjoint simulation.

Here, we formulate a general self-adjoint approach to the sensitivity analysis of network parameters [14]-[16]. It requires neither an adjoint problem

nor analytical system matrix derivatives. We focus on the linear problem in the method of moments, which is at the core of a number of commercial high-frequency simulators. Thus, for the first time, we suggest practical and fast sensitivity solutions realized entirely outside the framework of the EM solver. These standalone algorithms can be incorporated in an automated design to perform optimization, modeling, or tolerance analysis of high-frequency structures with any commercial solver, which exports the system matrix and the solution vector.

In the next section, we state the adjoint-based sensitivity formula and the definition of a self-adjoint problem. We then introduce the self-adjoint formulas for network-parameter sensitivity calculations. We outline the features of the commercial EM solvers, which enable independent network-parameter sensitivity analysis. Numerical validation and comparisons are presented in Section 3.5. Section 3.6 discusses the computational overhead associated with the sensitivity analysis. We give recommendations for further reduction of the computational cost whenever software changes are possible, and conclude with a summary.

3.2 FREQUENCY DOMAIN ADJOINT VARIABLE METHOD [14]

3.2.1 Sensitivities of Linear Complex Systems [14]

A time-harmonic EM problem involving linear materials can be cast in a linear system of complex equations by the use of a variety of numerical techniques:

$$\boldsymbol{A}\boldsymbol{x} = \boldsymbol{b} \tag{3.1}$$

The system matrix $\boldsymbol{A} \in \mathbb{C}^{M\times M}$ is a function of the shape and material parameters, some of which comprise the vector of designable parameters $\boldsymbol{p} \in \mathbb{R}^{N\times 1}$, i.e., $\boldsymbol{A}(\boldsymbol{p})$. Thus, the vector of state variables $\boldsymbol{x} \in \mathbb{C}^{M\times 1}$ is a function of $\boldsymbol{p}$, $\boldsymbol{x}(\boldsymbol{p})$. The right-hand side $\boldsymbol{b}$ results from the EM excitation and/or the inhomogeneous boundary conditions. Typically, in a problem of finding the sensitivities of network parameters, $\boldsymbol{b}$ is independent of $\boldsymbol{p}$, because the waveguide structures launching the incident waves (the ports) serve as a reference and are not a subject to design changes: $\nabla_{\boldsymbol{p}}\boldsymbol{b} = \boldsymbol{0}$.

For the purposes of optimization, the system performance is evaluated through a scalar real-valued objective function $F(\boldsymbol{x}, \boldsymbol{p})$. In tolerance analysis or model generation, we may consider a set of responses, some of which are complex. We first consider a single, possibly complex, function F, and we refer to it as the *response*. It is computed from the solution $\bar{\boldsymbol{x}}$ of (3.1) for a given design.

Through $\boldsymbol{x}$, F is an implicit function of $\boldsymbol{p}$. It may also have an explicit dependence on $\boldsymbol{p}$. Explicit dependence on a shape parameter p_i $(\partial^e F / \partial p_i \neq 0)$ arises when F depends on the field/current solution at points whose coordinates in

space are affected by a change in p_i. An example is the explicit dependence of an antenna gain on the position/shape of the wires [1] carrying the radiating currents. Explicit dependence with respect to a material parameter arises when F depends on the field/current solution at points whose constitutive parameters are affected by its change. An example is the stored energy in a volume of changing permittivity. The network parameters, however, are computed from the solution at the ports, whose shape and materials do not change. Thus, when F is a network parameter, $\nabla_{\boldsymbol{p}}^{e} F = \mathbf{0}$.

The derivatives of a complex response $F = F_R + jF_I$ ($j = \sqrt{-1}$) with respect to the design parameters $\boldsymbol{p} = [p_1 \cdots p_N]^T$ can be efficiently calculated using the adjoint-variable sensitivity formula [11][13]:

$$\frac{\partial F}{\partial p_i} = \frac{\partial^e F}{\partial p_i} + \hat{\boldsymbol{x}}^T \cdot \left(\frac{\partial \boldsymbol{b}}{\partial p_i} - \frac{\partial \boldsymbol{A}}{\partial p_i} \cdot \bar{\boldsymbol{x}} \right), \; i = 1, 2, \ldots, N . \tag{3.2}$$

In a compact gradient notation, (3.2) becomes

$$\nabla_{\boldsymbol{p}} F = \nabla_{\boldsymbol{p}}^{e} F + \hat{\boldsymbol{x}}^T \cdot \nabla_{\boldsymbol{p}} \left(\boldsymbol{b} - \boldsymbol{A}\bar{\boldsymbol{x}} \right) \tag{3.3}$$

We refer to $\nabla_{\boldsymbol{p}} F$ as the *response sensitivity*. The adjoint-variable vector $\hat{\boldsymbol{x}}$ is the solution to

$$\boldsymbol{A}^T \cdot \hat{\boldsymbol{x}} = (\nabla_{\boldsymbol{x}} F)^T_{\boldsymbol{x}=\bar{\boldsymbol{x}}} \tag{3.4}$$

where $\nabla_{\boldsymbol{x}} F$ is a row of the derivatives of F with respect to the state variables x_i, $i = 1, \ldots, M$, evaluated at the current solution $\boldsymbol{x} = \bar{\boldsymbol{x}}$. In the case of complex systems, it involves the real $\boldsymbol{x}_R$ and the imaginary $\boldsymbol{x}_I$ parts of the state variables.

As detailed in [13], the complex-response analysis (3.2)-(3.4) is valid if F is an analytic function of the state variables $\boldsymbol{x}$, in which case, the Cauchy-Riemann conditions [17] are fulfilled. A convenient form of the adjoint excitation $\hat{\boldsymbol{b}} = (\nabla_{\boldsymbol{x}} F)^T$ is

$$\hat{\boldsymbol{b}} = \left[\left(\frac{\partial F_R}{\partial x_{1_R}} + j \frac{\partial F_I}{\partial x_{1_R}} \right) \cdots \left(\frac{\partial F_R}{\partial x_{M_R}} + j \frac{\partial F_I}{\partial x_{M_R}} \right) \right]^T = (\nabla_{\boldsymbol{x}_R} F)^T = (\nabla_{\boldsymbol{x}} F)^T \tag{3.5}$$

3.2.2 Sensitivity Expression for Linear-network Parameters [14]

For a network parameter sensitivity, the gradients $\nabla_{\boldsymbol{p}} \boldsymbol{b}$ and $\nabla_{\boldsymbol{p}}^{e} F$ in (3.3) vanish, which leads to the sensitivity expression

$$\nabla_{\boldsymbol{p}} F = -\hat{\boldsymbol{x}}^T \cdot \nabla_{\boldsymbol{p}} \left(\boldsymbol{A} \bar{\boldsymbol{x}} \right). \tag{3.6}$$

We emphasize that in (3.6) $\bar{\boldsymbol{x}}$ is fixed, and only $\boldsymbol{A}$ is differentiated, as in (3.2).

The sensitivity formula (3.6) uses three quantities: the solution $\bar{\boldsymbol{x}}$ of the original problem (3.1), the set of system matrix derivatives $\partial \boldsymbol{A} / \partial p_i$, $i = 1, \ldots, N$, and the solution $\hat{\boldsymbol{x}}$ to the adjoint problem (3.4). The first one is available from the EM simulation. Also, we assume that the system matrix derivatives have been already computed, e.g., using finite differences [1] or Broyden's update [18][19]. We next show that in the case of the network parameters, the adjoint solution $\hat{\boldsymbol{x}}$ is equal to $\bar{\boldsymbol{x}}$ multiplied by a complex factor κ. Thus, the solution of (3.4) is unnecessary. We employ the above adjoint-variable theory to determine κ for different network parameters. For that, we also need to know the dependence of

the particular network parameter on the distributed field/current solution. We discuss this dependence below.

3.3 NETWORK PARAMETER SENSITIVITIES WITH CURRENT SOLUTIONS

3.3.1 Sensitivities of *S*-parameters

The *S*-parameters in the MoM depend on the current density solutions produced by the MoM solvers through simple linear relations. More specifically, the current solution at the ports is needed.

We implement our technique through FEKO® [20]. FEKO is primarily an antenna CAD software. It uses the EFIE for metallic objects, and the EFIE with specialized Green's functions for planar layered (printed) circuits. For dielectric objects, it uses a coupled field integral equation (PMCHW) technique. It also employs a fast multipole method (MLFMM) for large problems (does not support specialized Green's functions).

Consider the calculation of the *S*-parameters of a network of system impedance Z_0 by FEKO:

$$S_{kj} = \delta_{kj} - \frac{2Z_0 I_{k,j}}{V_j^e}, \ j,k = 1,\ldots,K. \tag{3.7}$$

Here, V_j^e is the *j*th port voltage source (usually set equal to 1) of internal impedance Z_0, and $I_{k,j}$ is the resulting current at the *k*th port when the *j*th port is

excited (the rest of the ports are loaded with Z_0). The right-hand side of (3.1) corresponding to V_j^e is $\boldsymbol{b}_j$.

If the structure consists of thin wires discretized into segments, the currents $I_{k,j}$ are the elements of the solution vector $\overline{\boldsymbol{x}}_j$ obtained with $\boldsymbol{b} = \boldsymbol{b}_j$. Then, each partial derivative

$$\frac{\partial S_{kj}}{\partial I_{k,j}} = -\frac{2Z_0}{V_j^e}, \ j,k = 1,\ldots,K \tag{3.8}$$

gives the only nonzero element of the respective adjoint excitation vector $\hat{\boldsymbol{b}}_{kj}$. Its position corresponds exactly to the position of the only nonzero element V_k^e of the original excitation at the kth port $\boldsymbol{b}_k$. This is because $I_{k,j}$ is computed at the very same segment where V_k^e is applied when the kth port is excited. Thus,

$$\hat{\boldsymbol{b}}_{kj} = -\frac{2Z_0}{V_k^e V_j^e}\boldsymbol{b}_k, \ j,k = 1,\ldots,K \tag{3.9}$$

If the structure and in particular its ports involve planar or curved metallic surfaces, FEKO applies triangular surface elements accordingly, and computes the surface current distribution [20]. In this case, each of the port currents is obtained from the current densities at the edge of its port:

$$I_{k,j} = \sum_{i \in \mathcal{S}_k} J_{k,j}^i \Delta l_k^i, \ j,k = 1,\ldots,K \tag{3.10}$$

where k denotes the port where the current is computed, and j denotes the port being excited. $J_{k,j}^i$ is the component of the surface current density normal to the

edge of the *i*th element of port *k* whose length is Δl_k^i. The current densities $J_{k,j}^i$, $i \in \mathcal{S}_k$, are elements of the solution vector $\boldsymbol{x}_j$, where $\mathcal{S}_k$ is the set of their indices.

We compute the elements of the adjoint excitation vector $\hat{\boldsymbol{b}}_{kj}$ as the derivatives of S_{kj} with respect to $J_{k,j}^i$, $i \in \mathcal{S}_k$:

$$[\hat{b}_{kj}]_i = \frac{\partial S_{kj}}{\partial J_{k,i}^{(j)}} = -\frac{2Z_0}{V_e^{(j)}} \cdot \Delta l_{k,i}\,,\ i \in \mathcal{S}_k\,. \tag{3.11}$$

All elements, for which $i \notin \mathcal{S}_k$, are zero.

On the other hand, the excitation vector $\boldsymbol{b}_k$, corresponding to the *k*th port excitation of the original problem, also has nonzero elements, whose indices are those in $\mathcal{S}_k$. Moreover, to ensure uniform excitation across the port, these excitation elements are equal to the applied excitation voltage V_k^e, scaled by the edge element Δl_k^i [21]:

$$[b_k]_i = V_k^e \cdot \Delta l_k^i\,,\ i \in \mathcal{S}_k\,. \tag{3.12}$$

Comparing (3.11) and (3.12), we conclude that the adjoint vectors $\hat{\boldsymbol{b}}_{kj}$ relate to the original excitation $\boldsymbol{b}^{(k)}$ as in (3.9).

If the MoM matrix fulfills the symmetry condition $\boldsymbol{A} = \boldsymbol{A}^T$, the adjoint solution vectors $\hat{\boldsymbol{x}}_{kj}$, $j,k = 1,\ldots,K$, obtained from the adjoint excitations $\hat{\boldsymbol{b}}_{kj}$ relate to the original solution vectors $\boldsymbol{x}_k$, $k = 1,\ldots,K$, as

$$\hat{\boldsymbol{x}}_{kj} = \kappa_{kj} \cdot \boldsymbol{x}_k \,,\ \kappa_{kj} = -\frac{2Z_0}{V_e^{(k)} V_e^{(j)}} \,. \tag{3.13}$$

However, the matrices arising in the large variety of MoM techniques are not always symmetric when a non-uniform unstructured mesh is used, which is the usual case. It would seem that in the case of an asymmetric MoM matrix, the solution of the adjoint problem is unavoidable. On the other hand, a linear EM problem is intrinsically reciprocal, and in the limit of an infinitely fine mesh, the MoM techniques tend to produce nearly symmetrical system matrices. In Section 3.7, we show an important result: if the mesh is fine enough to achieve a solution convergence error below 10 %, then the asymmetry of the system matrix is negligibly small as far as the sensitivity calculation is concerned. Consequently, the self-adjoint sensitivity analysis using (3.13) is adequate with a convergent MoM solution. Its sensitivities are practically indistinguishable from those produced by solving the adjoint problem.

To summarize the above theory, we state the sensitivity formula for the self-adjoint *S*-parameter problem:

$$\nabla_{\boldsymbol{p}} S_{kj} = -\kappa_{kj} (\bar{\boldsymbol{x}}_k)^T \cdot \nabla_{\boldsymbol{p}} \left(\boldsymbol{A} \bar{\boldsymbol{x}}_j \right),\ j,k = 1,\ldots,K \tag{3.14}$$

Here, κ_{kj} is a constant, which depends on the powers incident upon the *j*th and *k*th ports, as per (3.13).

3.3.2 Input Impedance Sensitivities

The *S*-parameters relate to all other types of network parameters through

known analytical formulas [22]. Thus, the *S*-parameter sensitivities can be converted to any other type of network-parameter sensitivities using chain differentiation.

On the other hand, the MoM is well suited for the computation of the input impedance Z_{in} of one-port structures, e.g., antennas. Input-impedance sensitivities have been already considered in [1], [18] and [19]. There, however, the self-adjoint nature of the problem has not been recognized. As a result, the implementation uses in-house MoM codes, which are modified to carry out the adjoint-problem solution.

Below, we give the coefficient κ in the self-adjoint sensitivity expression for Z_{in} computed with the MoM. Making use of the MoM port representation explained previously, the relation between the adjoint and the original excitation vectors is obtained as

$$\hat{\boldsymbol{b}} = -I_{in}^{-2} \cdot \boldsymbol{b} \tag{3.15}$$

regardless of whether the port consists of a single or multiple wire segments or metallic triangles. Thus, the self-adjoint sensitivity formula for Z_{in} is the same as (3.14) after replacing S_{kj} with Z_{in} and κ_{kj} with $-I_{in}^{-2}$. Here, I_{in} is the *complex* current at the port known already from the system analysis.

3.4 GENERAL PROCEDURE

Assume that the basic steps in the EM structure analysis have already been

carried out. These include:

(1) A geometrical model of the structure has been built through the graphic user interface of the simulator;

(2) A mesh has been generated;

(3) The system matrix $\boldsymbol{A}$ has been assembled;

(4) The system equations have been solved for all K port excitations, and the original solution vectors $\bar{\boldsymbol{x}}_k$, $k = 1, \ldots, K$, of the nominal structure have been found with sufficient accuracy.

The self-adjoint sensitivity analysis is then carried out with the following steps:

Step 1 Parameterization: identify design parameters p_i, $i = 1, \ldots, N$;

Step 2 Generation of matrix derivatives;

Step 3 Sensitivity computations: use (3.14) with the proper constant κ.

To get the derivative of the system matrix at Step 2, we perturb the structure slightly for each p_i, (with about 1 % of the nominal p_i value) while keeping the other parameters at their nominal values. We re-generate the system matrix $\boldsymbol{A}_i = \boldsymbol{A}(\boldsymbol{p} + \Delta p_i \cdot \boldsymbol{u}^i)$, where $\boldsymbol{u}^i$ is a $N \times 1$ vector whose elements are all zero except the ith one, $u_i = 1$. We compute the N derivatives of the system matrix via finite differences:

$$\frac{\partial \boldsymbol{A}}{\partial p_i} \approx \frac{\Delta \boldsymbol{A}}{\Delta p_i} = \frac{\boldsymbol{A}_i - \boldsymbol{A}}{\Delta p_i}, \; i = 1, \ldots, N \tag{3.16}$$

Note that (3.16) is applicable only if $\boldsymbol{A}$ and $\boldsymbol{A}_i$ are of the same size, i.e., the two respective meshes contain the same number of nodes and elements. Moreover, the numbering of these nodes and elements must correspond to the same locations (within the prescribed perturbation) in the original and perturbed structures.

3.5 SOFTWARE REQUIREMENTS AND IMPLEMENTATION IN FEKO

3.5.1 Software Requirements

The above steps show that the EM simulator must have certain features, which enable the self-adjoint sensitivity analysis.

(1) It must be able to export the system matrix so that the user can compute the system matrix derivatives with (3.16).

(2) It must allow some control over the mesh generation, so that (3.16) is physically meaningful.

(3) It must export the field/current solution vector so that we can compute the sensitivities with (3.14).

The second and third features are available with practically all commercial EM simulators. The first feature deserves more attention. In the MoM, the matrix is dense, and writing to the disk may be time consuming. Also, only a few of the commercial simulators give access to the generated system matrices. This is the

reason why our numerical experiments are carried out with FEKO. This solver is based on the MoM, and it has the option to export the system matrix to a file stored to the disk. It also exports the solution vector with the computed current distribution.

3.5.2 Implementation in FEKO

A. Data Extraction

FEKO provides a *PS* Card, which allows us to export the system matrix and the solution (current vector $\bar{\boldsymbol{I}}$). They are stored in **.mat* file and **.str* file, respectively. The **.mat* is a binary file, written on the Intel platform. It has a Fortran block structure using the double complex data type. We can read such data through MatLab. Special care must be taken:

1) Before we access the matrix, 19×4 bytes offsets must be skipped immediately after opening the binary files.
2) Each record is 8 bytes longer than the actual data (4 bytes before and 4 bytes after the data). So for instance for a matrix with 21×21 elements the length of the file is not $21\times21\times16 = 7056$ bytes (16 for double complex), but rather

$$\begin{aligned} & 21\times8 && \text{for each record} \\ +\ & 21\times21\times16 && \text{for the actual matrix} \\ =\ & 7224 \text{ bytes.} \end{aligned}$$

B. Mesh Control

FEKO defines its mesh by setting the maximum mesh edge size for each geometrical part. We could assign a different maximum mesh edge size for each part. Within each part, the size of the mesh edge is the same. For example, let the design parameter be the length of the microstrip line shown in Fig. 1. At the *i*th iteration, the length is L_i and at the (i + 1)th iteration, the length increases to L_{i+1}. We usually define the maximum size along the *y*-axis at the *i*th iteration as

$$\Delta L_{y_i} = \frac{L_i}{N}, \quad i = 1, 2, \ldots, n \tag{3.17}$$

where n is the maximum iteration number and N is the number of mesh edges along the *y*-axis.

In this definition, the number of mesh edges along the *y*-axis remains N, regardless of the value of L_i, see Fig. 3.1.

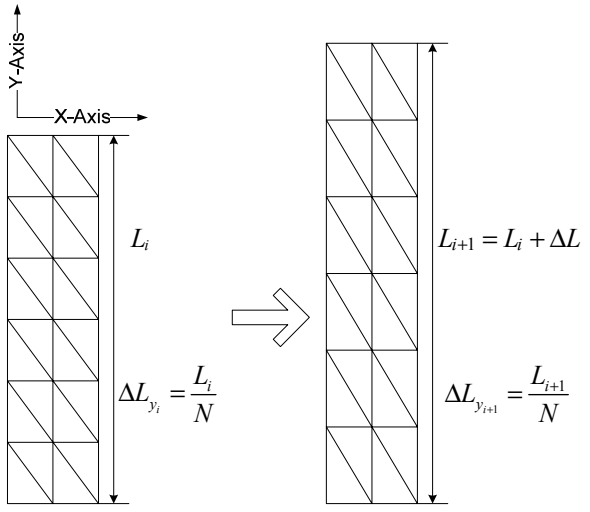

Fig. 3.1. Demonstration of mesh control in FEKO.

3.6 VALIDATION

We compute the network-parameter sensitivities with our self-adjoint formula and compare the results with those obtained by a forward finite-difference approximation applied directly at the level of the response. This second approach requires a full-wave simulation for each designable parameter. In all plots, our results are marked with SASA (for self-adjoint sensitivity analysis), while the results obtained through direct finite differencing are marked with FD. Our self-adjoint results are compared with the response derivatives obtained with the finite-difference approximation, which uses 1 % parameter perturbation.

3.6.1 Input Impedance Sensitivities of a Microstrip-Fed Patch Antenna

The microstrip-fed patch antenna [18] is printed on a substrate of relative dielectric constant $\varepsilon_r = 2.32$ and height $h = 1.59$ mm. The design parameters are its width W and length L shown in Fig. 3.2. The figure shows also the mesh of the metal layer. We compute the sensitivities of the antenna input impedance Z_{in}. Our derivatives with respect to the antenna length L ($45 \le L \le 55$ mm) for a width $W = 85$ mm and a frequency of 2.0 GHz are plotted together with the finite-difference results in Fig. 3.3.

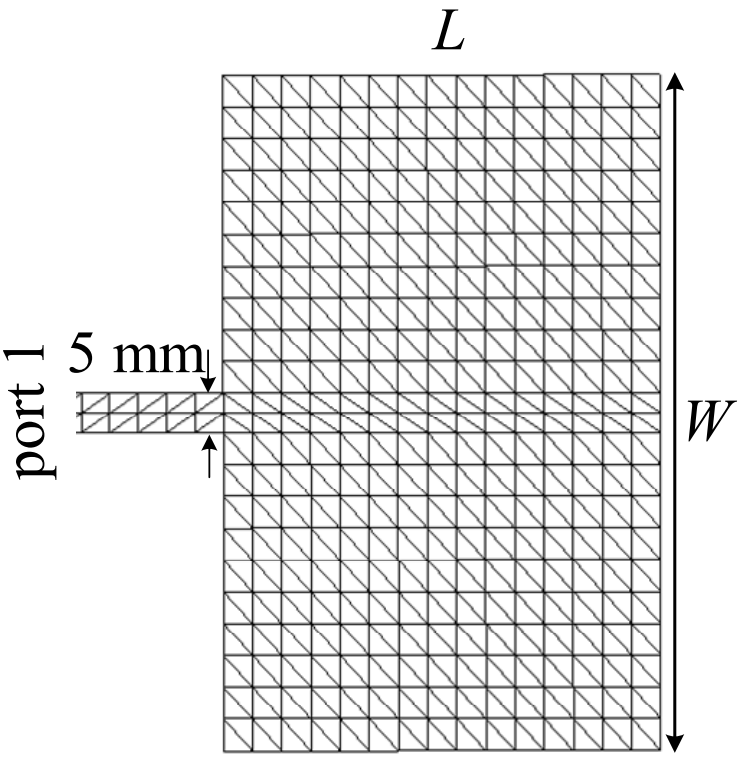

Fig. 3.2. Microstrip-fed patch antenna with design parameters $\boldsymbol{p} = [L \;\; W]^T$. The view shows the actual mesh.

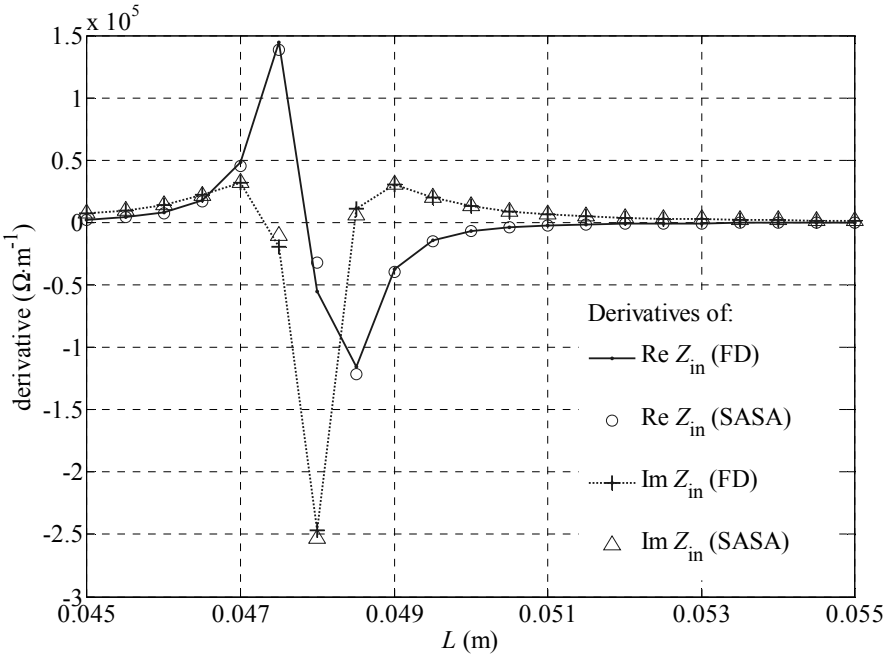

Fig. 3.3. Derivatives of Z_{in} with respect to the length L of the patch antenna at $f = 2.0$ GHz. The width is at $W = 85$ mm.

3.6.2 *S*-Parameter Sensitivities of the Bandstop Filter

This simple microstrip filter (Fig. 3.4) is printed on a substrate of $\varepsilon_r = 2.33$ and $h = 1.57$ mm. It is analyzed at $f = 4.0$ GHz. The design parameters are the width W and length L of the open-end stub. We compute the sensitivities of the *S*-parameter magnitudes and phases.

Note that the derivative of the phase ϕ of a complex response $|F|e^{j\phi} = F_R + jF_I$ is obtained from the derivatives of its real and imaginary parts:

$$\frac{\partial \phi}{\partial p} = |F|^{-2} \cdot \left(F_R \frac{\partial F_I}{\partial p} - F_I \frac{\partial F_R}{\partial p} \right) \tag{3.18}$$

Fig. 3.5 and Fig. 3.6 show the derivatives of $|S_{11}|$ and $|S_{21}|$ with respect to the stub length L when $W = 4.6$ mm.

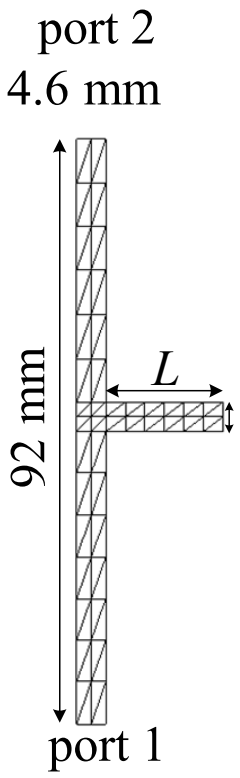

Fig. 3.4. Microstrip bandstop filter with design parameters $\boldsymbol{p} = [L \;\; W]^T$. The view shows the actual mesh.

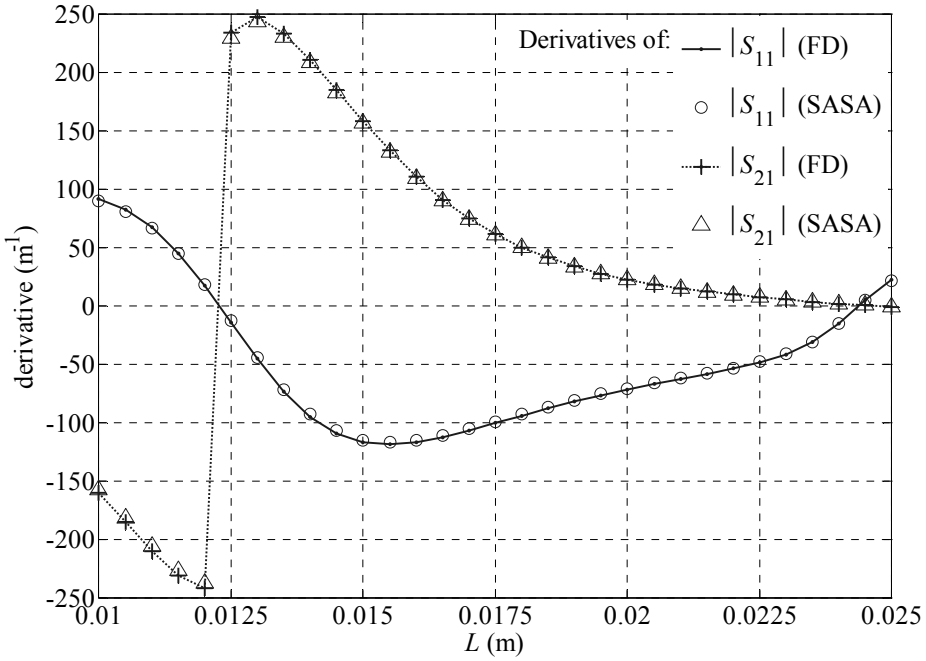

Fig. 3.5. Derivatives of the *S*-parameter magnitudes of the bandstop filter with respect to the stub length L at $f = 4.0$ GHz. The width is $W = 4.6$ mm.

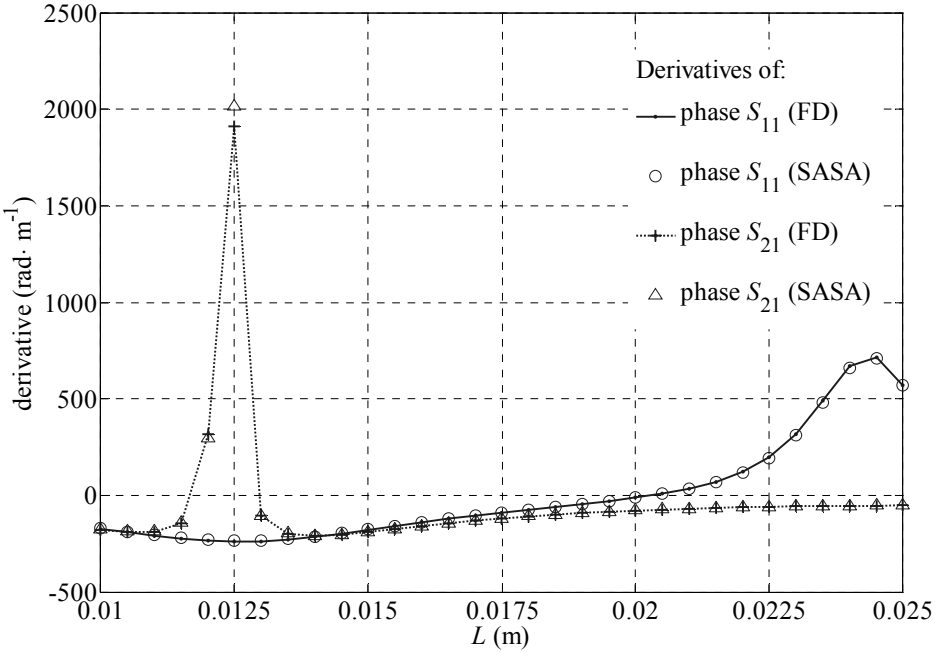

Fig. 3.6. Derivatives of the *S*-parameter phases of the bandstop filter with respect to the stub length L at $f = 4.0$ GHz. The width is $W = 4.6$ mm.

3.6.3 *S*-Parameter Sensitivities of the HTS Filter

We consider the high-temperature superconducting (HTS) bandpass filter of [23][24] (see the inset of Fig. 3.7). This filter is printed on a substrate with relative dielectric constant $\varepsilon_r = 23.425$, height $h = 0.508$ mm and substrate dielectric loss tangent of 3×10^{-5}. Design variables are the lengths of the coupled lines and the separations between them, namely, $\boldsymbol{p} = [S_1\ S_2\ S_3\ L_1\ L_2\ L_3]^T$. The length of the input and output lines is $L_0 = 1.27$ mm. The lines are of width $W = 0.1778$ mm. The filter is analyzed at $f = 4.0$ GHz. The derivatives of the system matrix are derived with 1 % perturbations. We compute the self-adjoint sensitivities of the S_{21} magnitude and phase, and compare it with the finite-difference approach with the same perturbations. Fig. 3.8 shows the derivatives of $|S_{21}|$ with respect to the spacing between the first coupled lines S_1 ($0.5 \le S_1 \le 0.75$ mm) when $[S_2\ S_3\ L_1\ L_2\ L_3]^T = [2.3764\ \ 2.6634\ \ 4.7523\ \ 4.8590\ \ 4.7490]^T$. Fig. 3.9 shows the derivatives of the respective phase. Good agreement is observed between the self-adjoint derivatives and the respective finite-difference estimates.

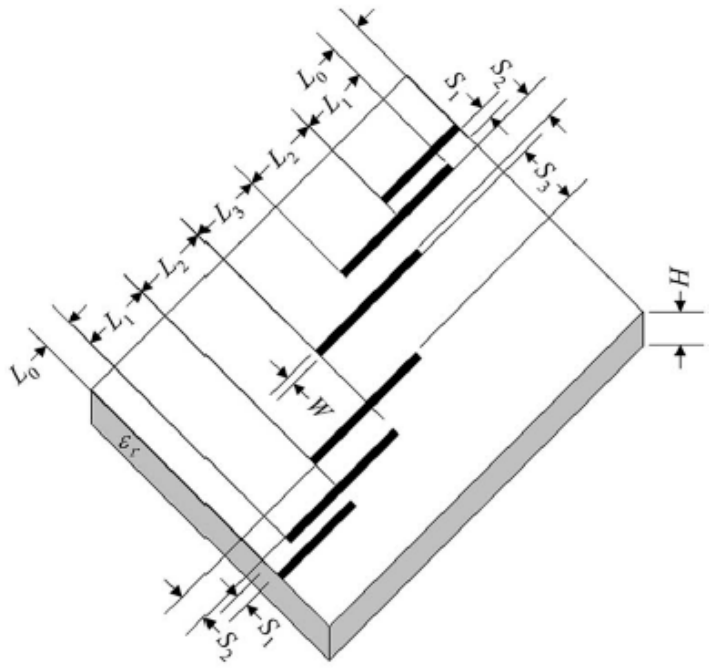

Fig. 3.7. The demonstration of the HTS filter [23].

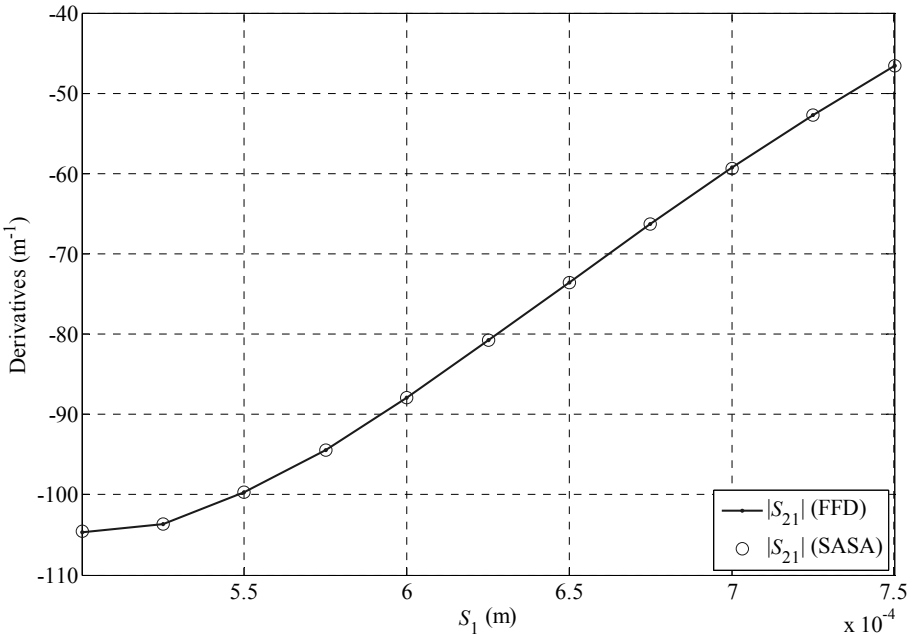

Fig. 3.8. Derivatives of $|S_{21}|$ with respect to S_1 at f=4.0 GHz for the HTS filter.

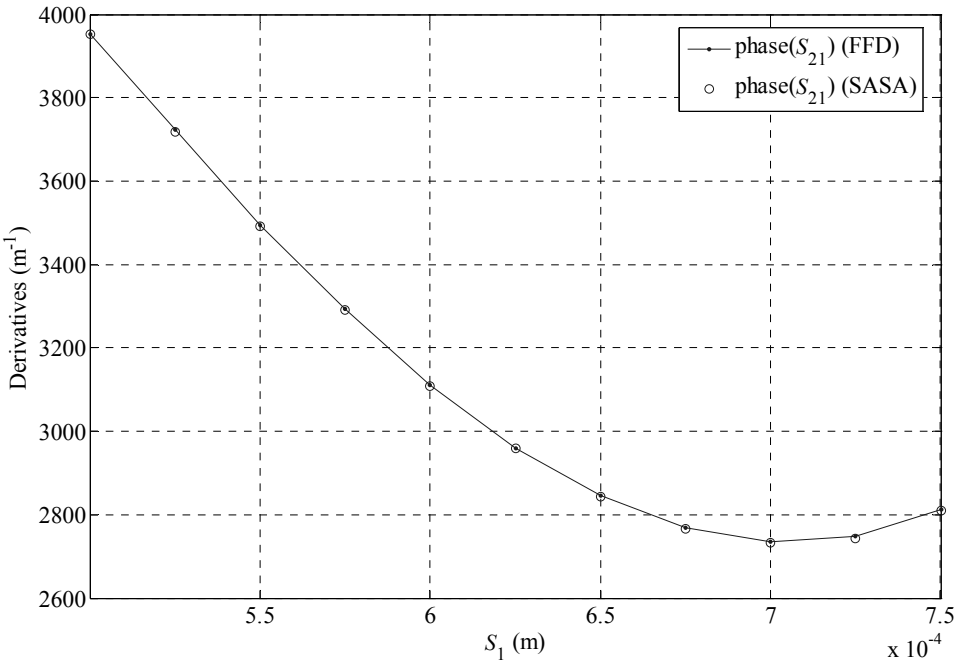

Fig. 3.9. Derivatives of $\varphi(S_{21})$ with respect to S_1 at f=4.0 GHz for the HTS filter in radians per meter.

3.7 DISCUSSION: MOM MATRIX SYMMETRY VERSUS CONVERGENCE OF SOLUTION

The self-adjoint sensitivities calculated with the MoM solver disregard the asymmetry of the system matrix as discussed in Section 3.3.1. In Table 3.1, we give quantitative assessment of this asymmetry in the two examples considered above in terms of three measures:

(a) maximum measure

$$a_{\max} = \max_{\substack{1\le i\le M \\ 1\le j\le M}} \left| \frac{A_{ij} - A_{ji}}{A_{ij}} \right| \tag{3.19}$$

(b) ℓ_1 measure

$$a_{\ell 1} = \frac{2}{M^2} \sum_{i=1}^{M-1} \sum_{j=i+1}^{M} \left| \frac{A_{ij} - A_{ji}}{A_{ij}} \right| \tag{3.20}$$

(c) ℓ_2 measure

$$a_{\ell 2} = \frac{1}{M^2} \sqrt{2 \sum_{i=1}^{M-1} \sum_{j=i+1}^{M} \left| \frac{A_{ij} - A_{ji}}{A_{ij}} \right|^2} \tag{3.21}$$

TABLE 3.1

ASYMMETRY MEASURES OF MOM MATRICES IN VALIDATION EXAMPLES

	patch antenna	bandstop filter
asymmetry measure $a_{\max}$	263	10.38
asymmetry measure $a_{\ell 1}$	0.3287	0.2333
asymmetry measure $a_{\ell 2}$	0.0012	0.0194

The excellent agreement between the self-adjoint sensitivities and the finite-difference sensitivities shown in Figs 3.3, 3.5 and 3.6 asserts that the asymmetry measures summarized in Table 3.1 are minor as far as the sensitivity calculations are concerned. We need, however, a robust criterion, which can assure the accuracy of the sensitivity result without the need to check against a reference.

We carry out the following experiment. We analyze the folded dipole shown in Fig. 3.10. The radius of the wire is $a = 10^{-4}\lambda$ and the spacing between the two wires is $s = 10^{-3}\lambda$. The length L varies from 0.2λ to 1.2λ. The response is the antenna input impedance Z_{in}. We force the maximum segment size on one of the two parallel wires to be 5 times larger than that on the other wire. This leads to very different segment lengths along the two parallel wires [see Fig. 3.10]. Since the two wires are very close, the MoM matrix is quite asymmetric. We emphasize that this is an abnormal (not recommended) segmentation allowing us to investigate a worst-case scenario. Normally, the user sets a global maximum segment length, which is applied to the entire structure, the result being a relatively uniform segmentation or mesh.

We next perform mesh refinement starting from a coarse mesh of 32 segments. Each iteration of the mesh refinement involves: 1) a decrease of the mesh elements by a certain factor, and 2) full-wave analysis with the current mesh. We decrease the maximum element size by approximately 50 % for each of the two parallel wires of the folded dipole. The ratio of 5 between them is preserved. The mesh refinement continues until a convergence error less than 1 % is achieved. The convergence error at the *k*th iteration is defined as

$$E^{(k)} = \frac{\left| Z_{in}^{(k)} - Z_{in}^{(k-1)} \right|}{\left| Z_{in}^{(k)} \right|} \cdot 100\,\% \tag{3.22}$$

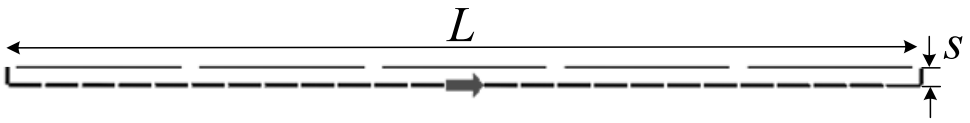

Fig. 3.10. The folded dipole and one of its coarse nonuniform segmentations in FEKO (32 segments). The radius of the wire is $a = 10^{-4}\lambda$ and the spacing between the wires is $s = 10^{-3}\lambda$. L is a design parameter, $0.2\lambda \le L \le 1.2\lambda$. The arrow in the center of the lower wire indicates the feed point.

TABLE 3.2

CONVERGENCE ERROR AND MATRIX ASYMMETRY MEASURES IN THE MESH REFINEMENT FOR THE FOLDED DIPOLE

iteration	1	2	3	4	5	6
segments	32	68	140	272	548	1088
E, %	N/A	25.99	9.665	1.918	1.097	0.8928
$a_{\ell 2}$	66.03	88.21	11.72	1.435	0.1101	0.0074
$a_{\ell 1}$	286.8	421.0	86.16	16.32	2.347	0.4261
$a_{\max}$	19887	91119	34588	11274	2425	1682

Here, $Z_{in}^{(k)}$ and $Z_{in}^{(k-1)}$ are the complex input impedances computed at the kth and $(k-1)$ st analyses. Convergence is achieved with a mesh of 1088 segments.

At each of the above analyses, we compute the matrix asymmetry measures, which are summarized in Table 3.2. We see that as soon as convergence is achieved, the asymmetry measures $a_{\ell 2}$ and $a_{\ell 1}$ become

comparable to those in the validation examples [see Table 3.1].

At every iteration of the mesh refinement, we also compute the derivative $\partial Z_{in}/\partial L$ (at $L = 0.5\lambda$) with our self-adjoint approach, i.e., ignoring the system matrix asymmetry. We compare the self-adjoint result for each mesh with its respective reference sensitivity. The reference sensitivity is computed with our original adjoint technique, which solves the adjoint problem, i.e., it fully accounts for the asymmetry of the system matrix. We define the asymmetry error in the computed response derivative D as

$$e_D = \frac{|D - \bar{D}|}{|\bar{D}|} \cdot 100 \ \% \tag{3.23}$$

where $\bar{D}$ is the reference derivative.

In Fig. 3.11, we plot the asymmetry derivative error e_D for $\partial Z_{in}/\partial L$ and the matrix asymmetry measure $a_{\ell 2}$ versus the convergence error E of the MoM solution [see (3.22)]. First, we see that $a_{\ell 2}$ increases as the convergence error E increases with a slope, which is very similar to that of e_D (unlike $a_{\ell 1}$ and $a_{\max}$). Apparently, $a_{\ell 2}$ is the matrix asymmetry measure, which can serve as a criterion for an accurate self-adjoint sensitivity calculation. As long as its value is below 2 %, we can expect e_D to be well below 1 %. Second, we conclude that as soon as an acceptable convergence is achieved in the response calculation ($E \leq 10$ %), we can have confidence in the self-adjoint response sensitivity calculation since its asymmetry error e_D is well below E, typically by two orders of magnitude.

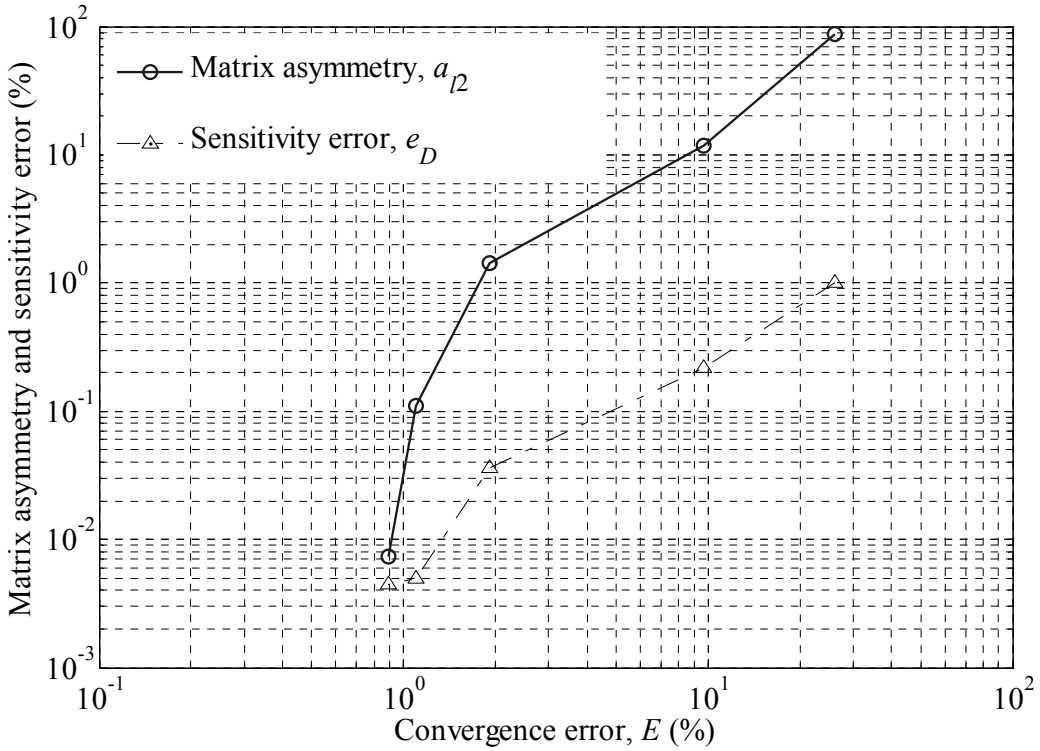

Fig. 3.11. The matrix asymmetry measure and the error of the computed derivative $\partial Z_{in} / \partial L$ (at $L = 0.5\lambda$) as a function of the convergence error of the analysis in the folded-dipole example.

In summary, if the MoM solution is setup properly and it yields network parameters of acceptable accuracy, it can be used to compute accurate network-parameter sensitivities with the self-adjoint approach. This approach is robust and insensitive to the asymmetry of the MoM system matrix.

For completeness, we note that our methodology is applicable when the MoM matrix is fully computed and is made accessible. The nature of the linear-system solver (direct or iterative) is unimportant in the self-adjoint analysis since an adjoint solution is not needed. However, MoM techniques based on fast

multipole expansions never fully compute the matrix and are thus not well suited for adjoint-based sensitivity analysis. For them, specialized adjoint-based algorithms need to be developed and, at this stage, applications with commercial solvers do not seem feasible. Response sensitivities with finite differences, however, are an option.

3.8 COMPUTATIONAL OVERHEAD OF THE SELF-ADJOINT SENSITIVITY ANALYSIS

The computational overhead associated with the self-adjoint sensitivity analysis is due to two types of calculations: 1) the system matrix derivatives, $\partial \boldsymbol{A} / \partial p_i$, $i = 1, \ldots, N$, and 2) the row-matrix-column multiplications involved in the sensitivity formula (3.14). Compared to the full-wave analysis, the sensitivity formula (3.14) requires insignificant CPU time, which is often neglected. We denote the time required to compute one derivative with the sensitivity formula as T_{SF}. In comparison, the calculation of the N system matrix derivatives is much more time consuming. Whether it employs finite differences or analytical expressions, it is roughly equivalent to N matrix fills. A matrix fill, especially in the MoM, can be time-consuming. We denote the time for one matrix fill as T_{MF}. Thus, the overhead time required by the self-adjoint sensitivity analysis is

$$T_{SASA} = N \cdot T_{MF} + N \cdot T_{SF} \tag{3.24}$$

On the other hand, if we employ forward finite differences directly at the

level of the response in order to compute the N derivatives of the network parameters, we need N additional full analyses, each involving a matrix fill and a linear system solution. Thus, the overhead of the finite-difference sensitivity analysis is

$$T_{FD} = N \cdot T_{MF} + N \cdot T_{LS} \tag{3.25}$$

where T_{LS} is the time required to solve (3.1).

The time cost comparison between the finite difference approach (FD), the adjoint variable method (AVM) and the self-adjoint sensitivity analysis (SASA) is given in Table 3.3.

TABLE 3.3

COMPARISON OF SENSITIVITY COMPUTATION OVERHEAD

	FD	AVM [1]	SASA
Matrix fills	$N \times T_{MF}$	$N \times T_{MF}$	$N \times T_{MF}$
Solving system equations	$N \times T_{LS}$	$1 \times T_{LS}$	0
Total	$N \times (T_{MF} + T_{LS})$	$N \times T_{MF} + T_{LS}$	$N \times T_{MF}$

We can define a time-saving factor as the ratio $S_T = T_{FD} / T_{SASA}$, which is a measure of the CPU savings offered by our sensitivity analysis approach:

$$S_T = \frac{T_{MF} + T_{LS}}{T_{MF} + T_{SF}} \tag{3.27}$$

Since T_{SF} is negligible in comparison with T_{MF},

$$S_T \approx 1 + \frac{T_{LS}}{T_{MF}} \tag{3.28}$$

Evidently, the larger the ratio $R = T_{LS} / T_{MF}$, the larger our time savings. Notice that $S_T \geq 1$, i.e., our approach would never perform worse than the finite-difference approach. R depends on the size of the problem—it grows as the number of unknowns M increases. This dependence is stronger in the MoM.

Fig. 3.12 shows the ratios $R = T_{LS} / T_{MF}$ of the FEKO solvers. The FEKO data is generated with a seven-element Yagi-Uda antenna [1][25] analyzed with increasingly finer segmentations whereby the number of unknowns increases from 240 to 11220. The plotted ratios are only representative since they depend on the type of the mesh (segments or triangles in FEKO) and on the type of the linear-system solver (direct or iterative). The trend of the ratio increasing with the size of the problem is general. We also emphasize that we record the CPU time only. With large matrices, a computer may run out of memory (RAM), in which case, part of the data is swapped to the disk. This causes a significant increase of T_{LS} and R, which is machine and hard-drive dependent. This is not taken into account.

In Table 3.4, we show the actual CPU time spent for response sensitivity calculations with our self-adjoint approach and the finite-difference approximation using the FEKO solver. We consider the case of one design parameter ($N = 1$), i.e., a single derivative is computed. The size of the system M varies. The increase of the time-saving factor S_T as the number of unknowns increases corresponds closely to the ratio curves $R = T_{LS} / T_{MF}$ plotted in Fig. 3.12 in accordance with (3.28). The analyzed structures are the same as those used to investigate the T_{LS} / T_{MF} ratios.

We also carry out a time comparison between our approach and the finite-difference approach when the size of the system M is fixed but the number of design parameters N varies. The MoM results are summarized in Table 3.5. As predicted by (3.28), the time savings are practically independent of the number of design parameters.

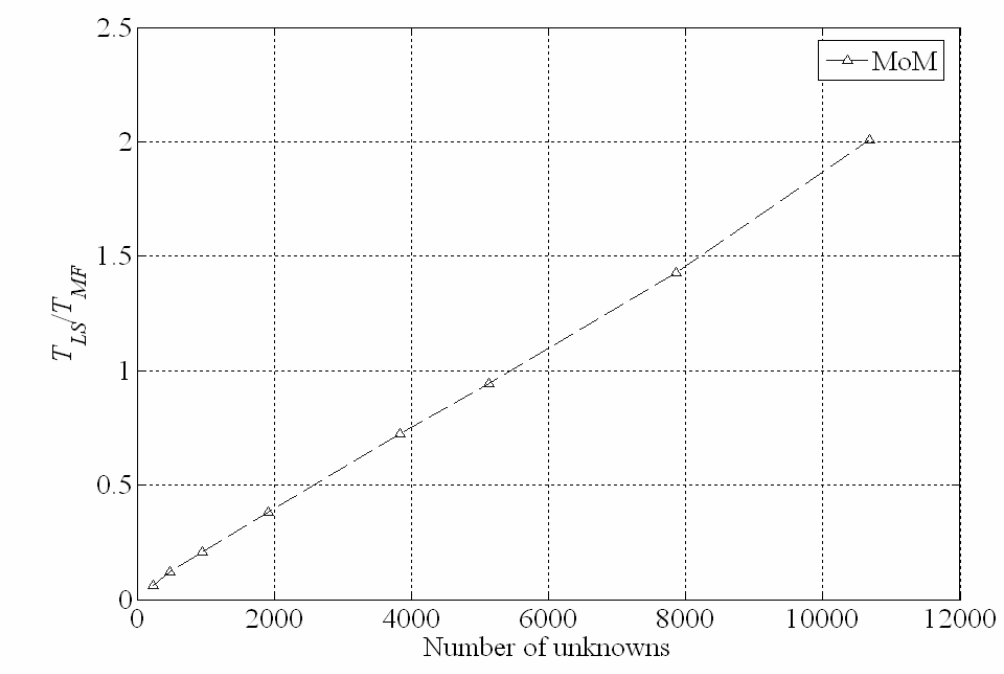

Fig. 3.12. The ratio between the time required to solve the linear system and the time required to assemble the system matrix in and FEKO (MoM).

TABLE 3.4

FEKO COMPUTATIONAL OVERHEAD OF SENSITIVITY ANALYSIS WITH SELF-ADJOINT METHOD AND WITH FINITE DIFFERENCES ($N = 1$)

M	240	480	960	1920	3840	7860	10680
T_{SASA} (s)	0.265	0.922	3.469	13.797	53.593	209.7	398.3
T_{FD} (s)	0.281	1.032	4.187	19.031	92.374	509.2	1188
S_T	1.060	1.119	1.207	1.379	1.724	2.429	2.983

TABLE 3.5

FEKO COMPUTATIONAL OVERHEAD OF SENSITIVITY ANALYSIS WITH SELF-ADJOINT METHOD AND WITH FINITE DIFFERENCES ($M = 10680$)

N	1	3	5	7	9	11
T_{SASA} (s)	398.34	1193.7	1988.0	2782.3	3576.4	4371.3
T_{FD} (s)	1188.3	3560.0	5925.8	8292.1	10660	13024
S_T	2.9831	2.9823	2.9808	2.9803	2.9807	2.9794

3.9 CONCLUDING REMARKS

We re-iterate that in optimization, the Broyden update is a far more efficient alternative to the computation of the system matrix derivatives [18][19][26]. With it, S_T becomes roughly proportional to $(T_{MF} + T_{LS})/T_{SF}$, which is normally a very large ratio. The application of this algorithm in optimization is to be discussed in the following chapter.

REFERENCES

[1] N.K. Georgieva, S. Glavic, M.H. Bakr, and J.W. Bandler, "Feasible adjoint sensitivity technique for EM design optimization," *IEEE Trans. Microwave Theory Tech.,* vol. 50, Dec. 2002, pp. 2751-2758.

[2] S. Amari, "Numerical cost of gradient computation within the method of moments and its reduction by means of a novel boundary-layer concept," *IEEE MTT-S Int. Microwave Symp*. *Digest*, 2001, pp.1945-1948.

[3] D.G. Cacuci, *Sensitivity & Uncertainty Analysis, Volume 1: Theory*. Boca Raton, FL: Chapman & Hall/CRC, 2003.

[4] A.D Belegundu and T.R. Chandrupatla, *Optimization Concepts and Applications in Engineering.* Upper Saddle River, NJ: Prentice-Hall, 1999.

[5] E.J. Haug, K.K. Choi, and V. Komkov, *Design Sensitivity Analysis of Structural Systems.* Orlando, FL: Academic, 1986.

[6] P. Neittaanmäki, M. Rudnicki, and A. Savini, *Inverse Problems and Optimal Design in Electricity and Magnetism*. New York: Oxford University Press, 1996, Chapter 4.

[7] Hong-bae Lee and T. Itoh, "A systematic optimum design of waveguide-to-microstrip transition," *IEEE Trans. Microwave Theory Tech*., vol. 45, May 1997, pp. 803-809.

[8] H. Akel and J.P. Webb, "Design sensitivities for scattering-matrix calculation with tetrahedral edge elements," *IEEE Trans. Magnetics*, vol. 36, July 2000, pp. 1043-1046.

[9] J.P. Webb, "Design sensitivity of frequency response in 3-D finite-element analysis of microwave devices," *IEEE Trans. Magnetics*, vol. 38, Mar. 2002, pp. 1109-1112.

[10] Y.S. Chung, C. Cheon, I.H. Park and S.Y. Hahn, "Optimal design method for microwave device using time domain method and design sensitivity analysis—part I: FETD case," *IEEE Trans. Magnetics*, vol. 37, Sep. 2001, pp. 3289-3293.

[11] N.K. Nikolova, J.W. Bandler and M.H. Bakr, "Adjoint techniques for sensitivity analysis in high-frequency structure CAD," *IEEE Trans. Microwave Theory Tech.*, vol. 52, Jan. 2004, pp. 403-419.

[12] S.M. Ali, N.K. Nikolova and M.H. Bakr, "Recent advances in sensitivity analysis with frequency-domain full-wave EM solvers," *Applied Computational Electromagnetics Society Journal*, vol. 19, Nov. 2004, pp. 147-154.

[13] M.H. Bakr and N.K. Nikolova, "An adjoint variable method for frequency domain TLM problems with conducting boundaries," *IEEE Microwave and Wireless Components Letters,* vol. 13, Sept. 2003, pp. 408-410.

[14] N.K. Nikolova, J. Zhu, D. Li, M.H. Bakr and J.W. Bandler, "Sensitivity analysis of network parameters with electromagnetic frequency-domain simulators," *IEEE Trans. Microwave Theory Tech*., vol. 54, Feb. 2006, pp. 670-681.

[15] J. Zhu, N.K. Nikolova and J. W. Bandler, "Self-adjoint sensitivity analysis of high-frequency structures with FEKO," the *22nd International Review of Progress in Applied Computational Electromagnetics Society* (*ACES* 2006), Miami, Florida, pp. 877-880.

[16] N.K. Nikolova, J. Zhu, D. Li and M.H. Bakr, "Extracting the derivatives of network parameters from frequency-domain electromagnetic solutions," the *XXVIIIth General Assembly of the International Union of Radio Science*, CDROM, Oct. 2005.

[17] M.D. Greenberg, *Advanced Engineering Mathematics*. Upper Saddle River, N.J.: Prentice Hall, 1998, pp. 1138-1140.

[18] N.K. Nikolova, R. Safian, E.A. Soliman, M.H. Bakr and J.W. Bandler, "Accelerated gradient based optimization using adjoint sensitivities," *IEEE Trans. Antennas Propagat*., vol. 52, Aug. 2004, pp. 2147-2157.

[19] E.A. Soliman, M.H. Bakr and N.K. Nikolova, "Accelerated gradient-based optimization of planar circuits," *IEEE Trans. Antennas Propagat*., vol. 53, Feb. 2005, pp. 880-883.

[20] FEKO® User's Manual, Suite 4.2, June 2004, EM Software & Systems-S.A. (Pty) Ltd, 32 Techno lane, Technopark, Stellenbosch, 7600, South Africa, http://www.feko.info. In the USA: EM Software & Systems (USA), Inc., 24 Research Drive, Hampton, VA 23666, USA, http://www.emssusa.com/.

[21] J. Zhu, "Sensitivity analysis of high-frequency structures with commercial software based on the method of moments," Computational Electromagnetics Res. Lab., McMaster University, CEM-R-23, June 2005.

[22] D. M. Pozar, *Microwave Engineering, 2nd ed.*, New York: John Wiley & Sons, 1998, Chapter 4.

[23] J.W. Bandler, R.M. Biernacki, S.H. Chen, W.J. Getsinger, P. A. Grobelny, C. Moskowitz and S.H. Talisa, "Electromagnetic design of high temperature superconducting microwave filters," *Int. J. RF Microwave Computer-Aided Eng.*, vol. 5, 1995, pp. 331-343.

[24] J.W. Bandler, Q.S. Cheng, N.K. Nikolova and M.A. Ismail, "Implicit space mapping optimization exploiting preassigned parameters," *IEEE Trans. Microw. Theory Tech*., vol. 52, no. 1, Jan. 2004, pp. 378-385.

[25] J. Zhu, "Time comparison and error estimation of the self-adjoint sensitivity analysis of network parameters with the method of moments," Computational Electromagnetics Res. Lab., McMaster University, CEM-R-24, June 2005.

[26] D. Li, J. Zhu, N.K. Nikolova, M.H. Bakr and J.W. Bandler, "EM optimization using sensitivity analysis in the frequency domain," submitted *to IEEE Trans. Antennas Propagat., Special Issue on Synthesis and Optimization Techniques in Electromagnetics and Antenna System Design*, Jan. 2007.

CHAPTER 4

EM OPTIMIZATION USING SENSITIVITY ANALYSIS IN THE FREQUENCY DOMAIN

4.1 INTRODUCTION

The previous implementation of the self-adjoint sensitivity analysis (SASA) technique provides us with accurate sensitivities in an efficient way. Sensitivities can be used for gradient-based optimization algorithms based on quasi-Newton, sequential quadratic programming (SQP) and trust-region methods, which need the objective function Jacobian and/or Hessian in addition to the objective function itself. These optimization methods search for a local optimal point. A gradient-based algorithm is expected to converge much faster, i.e., with fewer system analyses, than non-gradient optimization algorithms. Its drawback is that a global minimum is not guaranteed, and failure to converge is a possibility. Naturally, the solution provided by a gradient-based local optimization algorithm depends on the quality of the initial design. For a realistic

3D EM-based design problem with an acceptable starting point, gradient-based optimization is to be preferred [1].

The efficiency of a successful gradient-based optimization process depends mainly on two factors: (1) the number of the iterations required to achieve convergence, and (2) the number of simulation calls per iteration. The first factor depends largely on the nature of the algorithm, on the proper formulation of the objective or cost function, and the accuracy of the response Jacobians and/or Hessian. The second factor depends mostly on the method used to compute the Jacobians and/or Hessian, which are necessary to determine the search direction and the step in the design parameter space.

The sensitivity analysis, which provides the Jacobians through response-level approximations, is very time consuming. Our self-adjoint sensitivity analysis method [2]-[5] discussed in the last chapter, produces the response and its Jacobian with a single full-wave analysis when the objective function depends on the network parameters, e.g., the *S*-parameters and the input impedance. The major overhead of the sensitivity computation with this technique is due to the computation of the system matrix derivatives, whose overhead is equivalent to N matrix fills. N is the number of design parameters. A fast approach to the derivatives of the system matrix becomes necessary.

In this chapter, we firstly review the previous work related to the evaluation of the derivatives of the system matrix. Then, we propose a hybrid approach (B/FD-SASA) which employs both the finite-difference self-adjoint

sensitivity analysis (FD-SASA) method and Broyden-update self-adjoint sensitivity analysis (B-SASA) method. The latter is especially suitable for gradient-based EM optimization [1]. We develop a set of criteria for switching back and forth throughout the optimization process between the robust but more time-demanding FD-SASA and the B-SASA. This hybrid technique guarantees good accuracy of the gradient information with minimal computational time.

We implement our technique in the MoM through FEKO. We demonstrate our approach through the optimization of a double annular ring antenna. We compare its optimization performance with FD-SASA.

4.2 THE DERIVATIVES OF THE SYSTEM MATRIX [6]

In the self-adjoint sensitivity analysis, it is necessary to evaluate the derivatives of the system matrix with respect to all the design variables $\boldsymbol{p} = [p_1\ p_2\ \ldots\ p_n]^T$:

$$\frac{\partial \boldsymbol{A}}{\partial p_i}, \quad i = 1,\ 2,\ \ldots,\ n. \tag{4.1}$$

There are several ways to obtain the derivatives of the system matrix [6][7].

Method 1: The analytical derivatives of the system matrix $\boldsymbol{A}$ with respect to the design variables—if available—lead to exact response sensitivities. However, the analytical form of system matrix is hard to be determined in the general case.

Method 2: Forward finite differences give the simplest procedure. The sensitivities are calculated by:

$$\frac{\partial \boldsymbol{A}}{\partial p_i} = \frac{\boldsymbol{A}(\boldsymbol{p} + \boldsymbol{e}_i \Delta p_i) - \boldsymbol{A}(\boldsymbol{p})}{\Delta p_i}, \quad i = 1, 2 \ \ldots \ n \tag{4.2}$$

where

$$\boldsymbol{e}_i = \begin{bmatrix} 0 \\ \vdots \\ 1 \\ \vdots \\ 0 \end{bmatrix} i\text{th row} . \tag{4.3}$$

The self-adjoint sensitivity analysis using finite differences to evaluate the derivatives of the system matrix is referred to as FD-SASA. It provides accurate sensitivity and therefore is often used as a reference [2]-[5].

Method 3: The boundary-layer concept (BLC). The BLC in sensitivity analysis was first proposed by Amari [8]. It can be applied with solvers which allow non-uniform discretization and/or unstructured grids, e.g., the FEM and the MoM [7]. The idea is to perturb a certain geometrical parameter (the design parameter p_i) of a structure by respective deformations of as few grid elements as possible. This makes most of the system matrix coefficients insensitive to the perturbation. Consequently, the matrix derivative $\partial \boldsymbol{A} / \partial p_i$ is mostly sparse and only few nonzero coefficients need to be calculated. This is in contrast with Method 2, where full remeshing is applied to the perturbed structure, which

results in a full $\partial \boldsymbol{A} / \partial p_i$ matrix. In this method, we must have full control over the meshing.

Method 4: The Broyden update is discussed in Section 4.3.

4.3 SENSITIVITY ANALYSIS IN THE METHOD OF MOMENTS EXPLOITING THE BROYDEN UPDATE

Since in the FD-SASA the derivatives of the system matrix are computed with a finite-difference approximation, it requires at least N matrix fills. To eliminate this overhead, here, we compute the system matrix derivative applying Broyden's formula [9] to the elements of $\boldsymbol{A}$

$$\left(\frac{\partial \boldsymbol{A}}{\partial p_i}\right)^{(k+1)} = \left(\frac{\partial \boldsymbol{A}}{\partial p_i}\right)^{(k)} + \frac{\boldsymbol{A}(\boldsymbol{p}^{(k)}+\boldsymbol{h}^{(k)}) - \boldsymbol{A}(\boldsymbol{p}^{(k)}) - \sum_j \left(\frac{\partial \boldsymbol{A}}{\partial p_j}\right)^{(k)} h_j^{(k)}}{\boldsymbol{h}^{(k)T}\boldsymbol{h}^{(k)}} h_i^{(k)}, \; i=1,\ldots,N . \tag{4.4}$$

$\boldsymbol{A}(\boldsymbol{p}^{(k)})$ is the system matrix at the kth iteration, when the design parameter space is $\boldsymbol{p}^{(k)}$, and $\boldsymbol{h}^{(k)}$ is the increment vector in the design parameter space between the kth and (k+1)st iteration. The resulting sensitivity-analysis algorithm is referred to as B-SASA. With it, the derivatives of the system matrix in the first optimization iteration are obtained using a forward finite-difference approximation. They are updated iteratively thereafter. The iterative update requires negligible computational resources compared to a matrix fill.

4.4 MIXED SELF-ADJOINT SENSITIVITY ANALYSIS METHOD AND SWITCHING CRITERIA

The derivatives of the Broyden update are less accurate than those in the FD-SASA [7]. The inaccuracy tends to be significant when the increment of the design parameters is very small, e.g., near a local minimum, as catastrophic cancellation occurs. We propose two criteria to switch from B-SASA to FD-SASA:

1) $G(\boldsymbol{p}^{(k)}) > G(\boldsymbol{p}^{(k-2)})$, or

2) $\left\|\boldsymbol{h}^{(k)}\right\| \le d$.

Here G is the objective function and d is the minimum edge length of the mesh elements. The algorithm checks the criteria at each iteration. After a switch from B-SASA to FD-SASA occurs, only one optimization iteration is performed with the FD-SASA, after which the algorithm returns to B-SASA. This B/FD-SASA method is simple and guarantees acceptable accuracy of the system matrix derivatives even for small increments in the design-parameter space.

4.5 EXAMPLE: THE OPTIMIZATION OF A DOUBLE ANNULAR RING ANTENNA

We perform gradient-based optimization using the response Jacobian provided by: (1) the proposed hybrid B/FD SASA approach, (2) the FD-SASA. We compare the performance of the optimization algorithm with the three

sensitivity-analysis approaches in terms of the number of iterations and the overall CPU time.

We consider the stacked probe-fed printed annular ring antenna of [10], which is shown in Fig. 4.1. The simulations are performed with FEKO [11]. The antenna is printed on a printed circuit board (PCB) with $\varepsilon_{r1} = 2.2$, $d_1 = 6.096$ mm for the lower substrate, and $\varepsilon_{r2} = 1.07$, $d_2 = 8.0$ mm for the upper substrate. The dielectric loss tangent is 0.001 for both layers. The radius of the feed pin is $r_0 = 0.325$ mm. The design variables are the outer and inner radius of each ring and the feed position, namely, $\boldsymbol{p} = [a_1 \ a_2 \ b_1 \ b_2 \ \rho_p]^T$. The design specification is

$$|S_{11}| \le -10 \text{ dB} \quad \text{for } 1.75 \text{ GHz} \le f \le 2.15 \text{ GHz}.$$

Our technique requires the system matrix size fixed between iterations, regardless of the variation in the design parameters. It is realized by local meshing [12]. As shown in Fig. 4.2, the number of mesh edges along the five loops (thick lines) is topologically fixed at 13, 19, 25, 32 and 39, respectively.

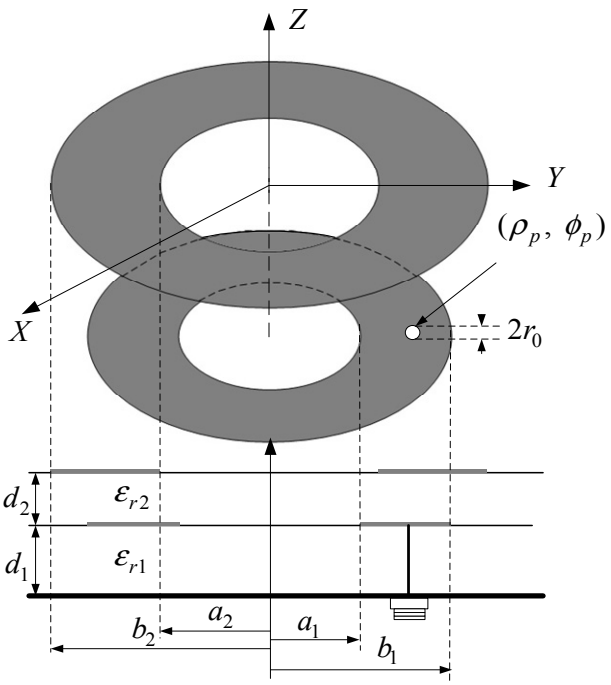

Fig. 4.1. Geometry of a stacked probe-fed printed double annular ring antenna [10].

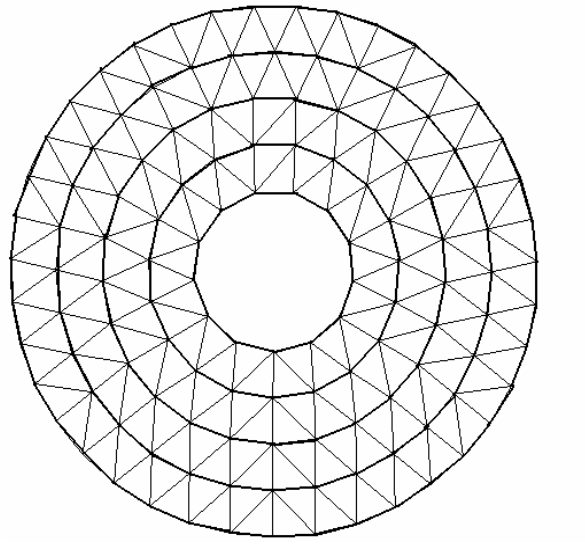

Fig. 4.2. Demonstration of local meshing of the stacked probe-fed printed double ring antenna.

We use Madsen's minimax optimization algorithm [13], which employs a trust region (TR). We supply the Jacobian calculated by our B/FD-SASA and FD-SASA techniques to the TR-minimax optimization algorithm. The initial trust-region size is set to $r_0 = 0.05 \cdot \|\boldsymbol{p}_0\|$. The starting point is $\boldsymbol{p}^{(0)}$=[a_1 a_2 b_1 b_2 ρ_p]=[30 30 20 10 10] (in mm). The algorithm switches to FD-SASA three times at the 4th, 9th and 10th iterations. The optimal designs for both approaches are reached within 11 iterations. The optimal designs emerge as $\boldsymbol{p}^{*(11)}_{\text{B/FD-SASA}}$ = [33.139 28.836 18.592 9.9592 8.8593] (in mm) and $\boldsymbol{p}^{*(11)}_{\text{FD-SASA}}$ = [33.088 28.992 18.437 9.849 8.5712] (in mm).

Figs. 4.3 and 4.4 show the parameters step size and the objective function, respectively, versus iterations. Fig. 4.5 shows the responses at the initial design and the optimal designs obtained with the Jacobians being provided by the B/FD-SASA and the FD-SASA. It is clear that both designs are practically identical. The overall time cost for the optimization with the B/FD-SASA is 2115 s versus 4358 s for the FD-SASA optimization. Again, significant time saving is observed.

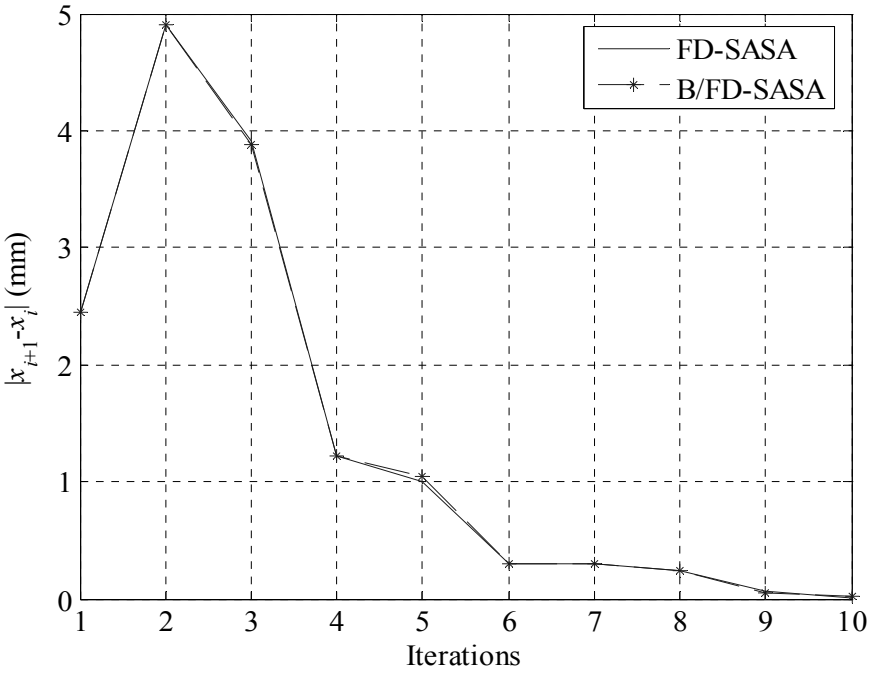

Fig. 4.3. Parameter step size vs. optimization iterations using TR-minimax in the double annular ring example.

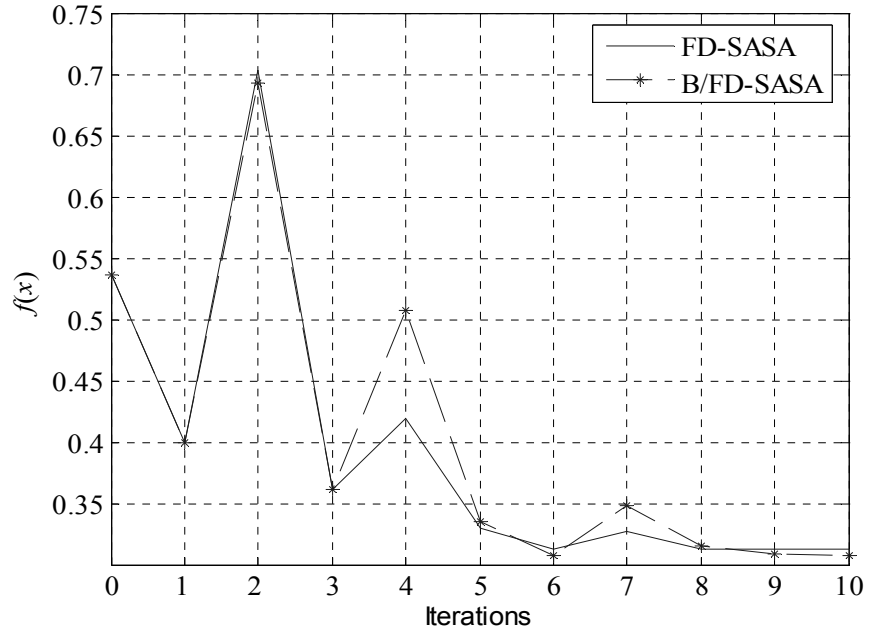

Fig. 4.4. Objective function vs. optimization iterations using TR-minimax in the double annular ring example.

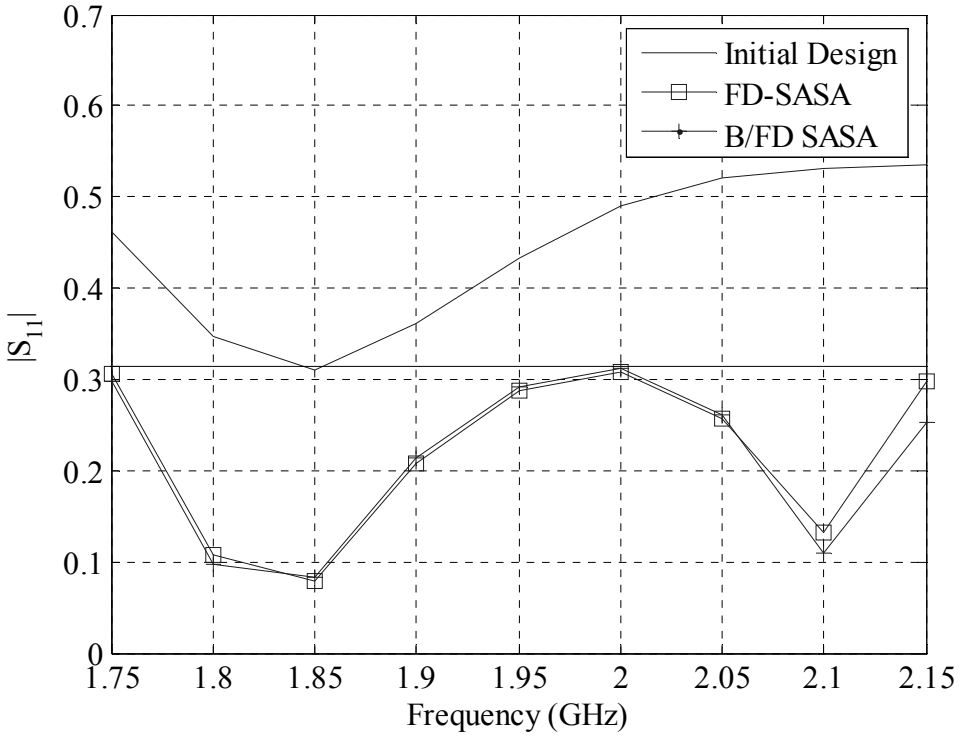

Fig. 4.5. Responses at the initial design and the optimal designs in the double annular ring example.

4.6 CONCLUDING REMARKS

The proposed hybrid technique of B/FD-SASA solves the EM optimization problem with a derivative approximation at the system matrix level. It significantly reduces the CPU time cost of the sensitivity computation. The time savings depend on the optimization algorithms, as well as on the numerical size of the problem. For electrically large 3-D problems with many design parameters, the time savings may be significant.

REFERENCES

[1] D. Li, J. Zhu, N.K. Nikolova, M.H. Bakr and J.W. Bandler, "EM optimization using sensitivity analysis in the frequency domain," submitted to *IEEE Trans. Antennas Propagat., Special Issue on Synthesis and Optimization Techniques in Electromagnetics and Antenna System Design*, Jan. 2007.

[2] N.K. Nikolova, J. Zhu, D. Li, M.H. Bakr and J.W. Bandler, "Sensitivity analysis of network parameters with electromagnetic frequency-domain simulators," *IEEE Trans. Microwave Theory Tech*., vol. 54, Feb. 2006, pp. 670-681.

[3] D. Li and N. K. Nikolova, "*S*-parameter sensitivity analysis of waveguide structures with FEMLAB," *COMSOL Multiphysics Conf.*, Cambridge, MA, Oct. 2005, pp. 267-271.

[4] J. Zhu, N.K. Nikolova and J. W. Bandler, "Self-adjoint sensitivity analysis of high-frequency structures with FEKO," the *22nd International Review of Progress in Applied Computational Electromagnetics Society* (*ACES 2006*), Miami, Florida, pp. 877-880.

[5] N.K. Nikolova, J. Zhu, D. Li and M.H. Bakr, "Extracting the derivatives of network parameters from frequency-domain electromagnetic solutions," *the XXVIIIth General Assembly of the International Union of Radio Science*, Oct. 2005.

[6] R. Safian, "Electromagnetic design sensitivity analysis exploiting the Broyden update," Master Thesis, Department of Electrical and Computer Engineering, McMaster University.

[7] N.K Nikolova, R. Safian, E.A. Soliman, M.H. Bakr and J.W. Bandler, "Accelerated gradient based optimization using adjoint sensitivities," *IEEE Trans. Antenna Propagat.* vol. 52, Aug. 2004, pp. 2147-2157.

[8] S. Amari, "Numerical cost of gradient computation within the method of moments and its reduction by means of a novel boundary-layer concept," in *Proc. IEEE MTT-S Int. Symp. Dig.*, vol. 3, 2001, pp. 1945-1948.

[9] C. G. Broyden, "A class of methods for solving nonlinear simultaneous equations," *Mathematics of Computation*, vol. 19, 1965, pp. 577-593.

[10] D. M. Kotokoff, J. T. Aberle and R. B. Waterhouse, "Rigorous analysis of probe-fed printed annular ring antennas," *IEEE Trans. Antennas Propagat*, vol. 47, Feb. 1999, pp. 384-388.

[11] FEKO® , *User's Manual*, Suite 4.2, June 2004, EM Software & Systems-S.A. (Pty) Ltd, 32 Techno Lane, Technopark, Stellenbosch, 7600, South Africa.

[12] "Mesh refinement," *FEKO Quarterly*, Dec. 2004.

[13] J.W. Bandler, W. Kellerman and K. Madsen, "A superlinearly convergent minimax algorithm for microwave circuit design," *IEEE Trans. Microwave Theory Tech.*, vol. MTT-33, Dec. 1985, pp. 1519-1530.

PART II

ANTENNA OPTIMIZATION THROUGH SPACE MAPPING

CHAPTER 5

ANTENNA DESIGN THROUGH SPACE MAPPING OPTIMIZATION

5.1 INTRODUCTION

The method of moments (MoM) is one of the most popular numerical techniques for antenna and microwave device analysis. An accurate MoM simulation is CPU intensive. This cost may be prohibitive for complex design problems. Alternatively, a coarse mesh MoM simulation is fast but poor in accuracy.

The space mapping (SM) technique takes advantage of the efficiency of a coarse mesh MoM simulation and the accuracy of the fine mesh simulation. SM aligns coarse models with fine models [1]-[8]. Here, the fine model is the fine mesh MoM solution. The coarse model is the coarse mesh solution.

For the first time, we apply the SM technique to antenna design. Both fine and coarse models are defined within FEKO [9]. We propose a new meshing method. The topology of the mesh is preserved throughout the optimization which

makes the coarse-model response in the design parameter space smooth and consistent.

In the parameter extraction (PE) process, we implement implicit/input SM and output SM sequentially [10]. In a preliminary PE, we roughly align the coarse model with the fine model through implicit/input SM. Then output SM aims at locally matching the surrogate with the fine model.

The novel SMF (Space Mapping Framework) system [11] implements our approach. SMF is a prototype GUI (Graphical User Interface) oriented software package that implements a number of SM optimization algorithms. The system aims at making SM accessible to engineers inexperienced in space mapping. It provides sockets to popular simulators (including FEKO, Sonnet ***em*** and ADS) that allow automatic fine/coarse model data acquisition and, consequently, fully automatic space mapping optimization. SMF also provides interfaces for SM modeling and statistical analysis.

Two examples are given to demonstrate our approach. We consider a double annular ring antenna and a patch antenna. In the first example, we exploit the CPU-intensive surface equivalence principle (SEP) as a fine model and the special Green's function with a coarse mesh as a coarse model. The *S*-parameter response is optimized in three iterations. In the second example, we optimize impedance at a single frequency using two SM plans. The comparisons show a larger time saving in SM plan I. At last, we discuss the coarseness in the coarse model and its effect on the SM performance.

5.2 COARSE MODEL AND FINE MODEL

As we discussed in Section 2.3, the mesh convergence needs to be checked to get an accurate simulation result. This is done by refining the mesh from one simulation to the next, and keeping all model parameters the same. If the results are significantly different, the antenna surfaces are not adequately discretized and we need to refine the mesh [12].

The coarse-mesh coarse model does not need to achieve mesh convergence. Consequently, if the mesh topology and number of mesh elements vary due to the variation of geometrical design parameters during optimization, inconsistent results are obtained. To overcome this problem, we force the mesh number and topology to remain unchanged during optimization. This is done by local meshing in FEKO.

In the fine model, where mesh convergence is satisfied, we use global meshing. We define the mesh density by the number of meshes per wavelength.

5.3 SPACE MAPPING-BASED SURROGATE MODELS [7][8]

5.3.1 Mathematical Formulations

We are concerned with a class of optimization algorithms that exploit surrogate models [13]. Let $\boldsymbol{R}_f : X_f \to R^m$ denote the response vector of the so-called fine model of a given object, where $X_f \subseteq R^n$. Our goal is to solve

$$\boldsymbol{x}_f^* = \arg \min_{\boldsymbol{x}_f \in X_f} U(\boldsymbol{R}_f(\boldsymbol{x}_f)) \tag{5.1}$$

where U is a suitable objective function.

SM assumes the existence of a less accurate but much faster coarse model. Let $\boldsymbol{R}_c : X_c \times X_p \to R^m$ denote the response vectors of the coarse model, where $X_c \subseteq R^n$ is the design variable domain (we assume here that $X_c \subseteq X_f$) and $X_p \subseteq R^q$ is the domain of auxiliary (preassigned) coarse model parameters. Typical preassigned parameters $\boldsymbol{x}_p$ are the dielectric constant and the height of a dielectric layer. By $\boldsymbol{x}_c^*$ we denote the optimal solution of the coarse model, i.e.,

$$\boldsymbol{x}_c^* \triangleq \arg \min_{\boldsymbol{x} \in X_c} U(\boldsymbol{R}_c(\boldsymbol{x}, \boldsymbol{x}_p^{(0)})) \tag{5.2}$$

where $\boldsymbol{x}_p^{(0)}$ denotes the initial preassigned parameter values.

We consider the fine model to be expensive to compute and solving (5.1) by direct optimization to be impractical. Instead, we use surrogate models, i.e., models that are not as accurate as the fine model but are computationally cheap,

hence suitable for iterative optimization. We consider an optimization algorithm that generates a sequence of points $\boldsymbol{x}_f^{(i)} \in X_f,\ i = 1, 2, \ldots,$ so that

$$\boldsymbol{x}_f^{(i+1)} = \arg\min_{\boldsymbol{x} \in X_c} U(\boldsymbol{R}_s^{(i)}(\boldsymbol{x})). \tag{5.3}$$

Here, $\boldsymbol{R}_s^{(i)} : X_c \rightarrow R^m$ is the surrogate model at iteration *i*, which uses the coarse model and the fine model data.

In this work, we use a surrogate model based on input SM [13], implicit SM [2] and output SM [3]. The surrogate model at iteration *i* is defined as

$$\boldsymbol{R}_s^{(i)}(\boldsymbol{x}) = \boldsymbol{R}_c(\boldsymbol{B}^{(i)}\boldsymbol{x} + \boldsymbol{c}^{(i)}, \boldsymbol{x}_p^{(i)}) + \boldsymbol{\Delta R}^{(i)} \tag{5.4}$$

where

$$(\boldsymbol{B}^{(i)}, \boldsymbol{c}^{(i)}, \boldsymbol{x}_p^{(i)}) = \arg\min_{(\boldsymbol{B}, \boldsymbol{c}, \boldsymbol{x}_p)} \varepsilon^{(i)}(\boldsymbol{B}, \boldsymbol{c}, \boldsymbol{x}_p) \tag{5.5}$$

and

$$\boldsymbol{\Delta R}^{(i)} = \boldsymbol{R}_f^{(i)}(\boldsymbol{x}_f^{(i)}) - \boldsymbol{R}_c(\boldsymbol{B}^{(i)}\boldsymbol{x}_f^{(i)} + \boldsymbol{c}^{(i)}, \boldsymbol{x}_p^{(i)}) \tag{5.6}$$

The matrices $\boldsymbol{B}^{(i)} \in M_{n \times n}$, $\boldsymbol{c}^{(i)} \in M_{n \times 1}$, and the vector $\boldsymbol{x}_p^{(i)}$ are obtained using parameter extraction applied to the matching condition $\varepsilon^{(i)}$. Vector $\boldsymbol{\Delta R}^{(i)} \in M_{m \times 1}$ is calculated using formula (5.6) after having determined $\boldsymbol{B}^{(i)}$, $\boldsymbol{c}^{(i)}$ and $\boldsymbol{x}_p{}^{(i)}$. A general form of the matching condition is

$$\varepsilon^{(i)}(\boldsymbol{B}, \boldsymbol{c}, \boldsymbol{x}_p) = \sum_{k=0}^{i} w_k \,\|\, \boldsymbol{R}_f(\boldsymbol{x}_f^{(k)}) - \boldsymbol{R}_c(\boldsymbol{B} \cdot \boldsymbol{x}_f^{(k)} + \boldsymbol{c}, \boldsymbol{G} \cdot \boldsymbol{x}_f^{(k)} + \boldsymbol{x}_p) \,\| \tag{5.7}$$

In our examples we use w_1=1 and w_k=0, k=2,…,i (i.e., we only use the last iteration point to match the models).

Both implicit, input and output SM aim at reducing the misalignment between the fine model and the current surrogate, however, implicit and input SM exploit the physics-based similarity of the models, while the output SM ensures perfect local alignment between the models at the current iteration point. As follows from equations (5.4)-(5.7), we implement implicit/input SM and output SM sequentially. This is illustrated in Fig. 5.1.

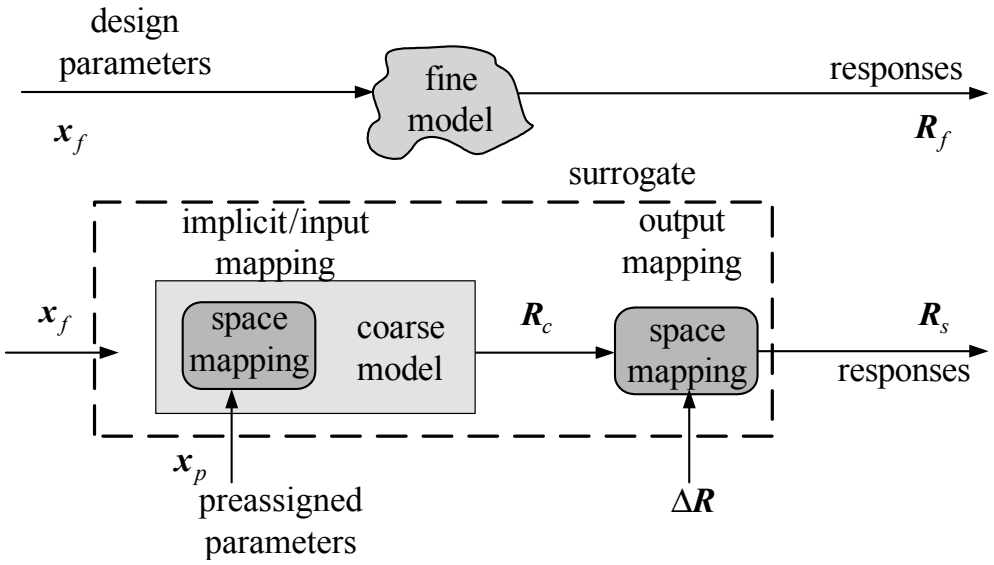

Fig. 5.1. Demonstration of our approach to implicit, input and output SM.

5.3.2 Algorithm

Having defined the family of surrogate models we can define the optimization algorithm. It is, in fact, an implementation of the generic surrogate model-based optimization algorithm (5.3):

Step 1 Choose a proper coarse-mesh coarse model as well as preassigned parameters. Set $i = 0$.

Step 2 Solve (5.2) to find the surrogate optimal solution $\boldsymbol{x}_c^*$ and let $\boldsymbol{x}_f^{(0)} = \boldsymbol{x}_c^*$.

Step 3 Evaluate the fine model to find $\boldsymbol{R}_f(\boldsymbol{x}_f^{(i)})$.

Step 4 Update the surrogate model $\boldsymbol{R}_s^{(i)}$ according to (5.4)-(5.6).

Step 5 Solve (5.3) and obtain $\boldsymbol{x}_f^{(i+1)}$.

Step 6 If the termination condition is satisfied (convergence achieved or the design specification satisfied.), stop; otherwise, set $i = i+1$ and go to Step 3.

5.4 SMF: SPACE MAPPING FRAMEWORK [11]

5.4.1 Brief Introduction to SMF

SMF [11] is designed to make space mapping accessible to engineers not experienced in this technology. It is a GUI based Matlab system that can perform space mapping based constrained optimization, modeling and statistical analysis. It implements existing SM approaches, including input, output, implicit and frequency SM. It contains drivers for commercial simulators (Sonnet ***em***, MEFiSTo, ADS, FEKO) that allow linking of the fine/coarse model to the algorithm and to make the optimization process fully automatic.

5.4.2 SMF Design Flow

In this thesis, we only focus on one aspect of SMF, a module for automatic space mapping optimization. We have used it to solve the example antenna design problems considered in Chapter VI.

Fig. 5.2 shows a block diagram of the optimization module in SMF. Optimization is performed in several steps. First, the user enters problem arguments, including starting point, frequency sweep, optimization type and specifications. Next, the user sets up space mapping itself, i.e., the kind of space mapping to be used (e.g., input, output, implicit), specifies the termination condition, parameter extraction options, and optional constrains.

The next step is to link the fine and coarse models to SMF by setting up the data that will be used to create model drivers. Using the user-provided data (e.g., simulator input files and design variable identification data), SMF creates drivers that are later used to evaluate fine/coarse models for any necessary design variable values. Model evaluation is accomplished by generating the simulator input file corresponding to the required design, running the simulator and acquiring the results.

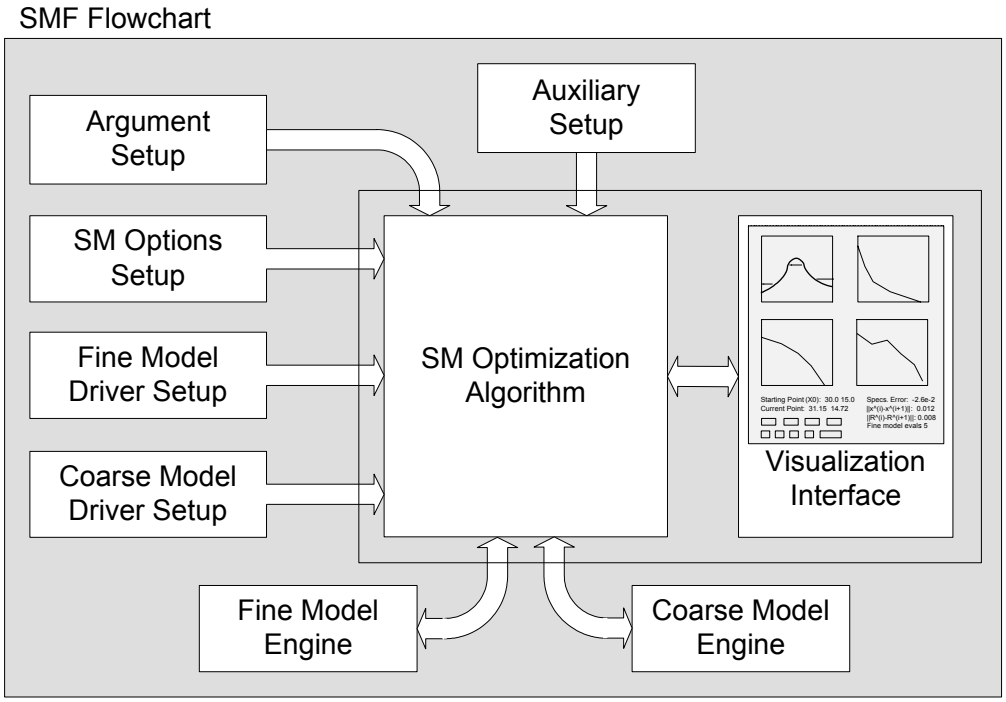

Fig. 5.2. Flowchart of the optimization module in the SMF system [11].

Parameter extraction, surrogate model optimization and optional trust region specific options are set in the next step using auxiliary interfaces.

Having done the setup, the user runs the execution interface, which allows the execution of the space mapping optimization algorithm and visualization of the results. The latter includes model responses, specification error plots as well as convergence plots.

5.5 EXAMPLES

5.5.1 Double Annular Ring Antenna

We consider the stacked probe-fed printed annular ring antenna of [14], which is shown in Fig. 4.1. The antenna is printed on a PCB with $\varepsilon_{r1} = 2.2$, $d_1 = 6.096$ mm for the lower substrate and $\varepsilon_{r2} = 1.07$, $d_2 = 8.0$ mm for the upper substrate. The dielectric loss tangent is 0.001 for both layers.

Note that in this example, finite ground is used. The finite ground size is 100×100 mm. The radius of the feed pin is $r_0 = 0.325$ mm. Design variables are the outer and inner radius of each ring and the feed position, namely, $[a_1 \ a_2 \ b_1 \ b_2 \ \rho_p]^T$. The design specification is

$$|S_{11}| \le -10 \text{ dB} \quad \text{for } 1.75 \text{ GHz} \le \omega \le 2.15 \text{ GHz}.$$

In an MoM solver like FEKO, special Green's functions are usually implemented to model multi-layer substrates, where the ground and the substrate are assumed infinite in extent. It is computer-resource efficient, since only the finite metallic surfaces are discretized. However, in many microwave and RF applications, the infinite ground plane assumption is not acceptable for accurate simulations. The ground size has a strong effect on the performance of microstrip antennas [15][16].

The surface equivalence principle (SEP) addresses this problem. The surface of a dielectric is discretized and both the electric and magnetic surface

currents are computed. All sides of a dielectric have to be meshed, making a closed solid. In this approach, the memory requirement is four times what it would be if the same structure was metallic [17]. A detailed discussion can be found in Section 2.4.

We choose the SEP model as the fine model and the special Green's function, which does not consider the finite ground size effect, as the coarse model. To further reduce the simulation time in the coarse model, we apply a coarser mesh by local meshing. As shown in Fig. 5.3, the number of mesh edges along the three loops (thick lines) is topologically fixed at 5, 10 and 15, respectively, regardless of the variation in the design parameter values. The detailed fine and coarse models are summarized in Table 5.1.

Here, we show how to set up and run the SM optimization for this problem using SMF. Fig. 5.4 shows the direct coarse model optimization interface, which was used to find the starting point for the SM optimization of the fine model. Fig. 5.5 shows the setup of the starting point, the frequency sweep, the optimization type and specifications within SMF. Fig. 5.6 shows the space mapping options interface. Here, the user can set up the termination conditions of the algorithm in terms of maximum number of iterations or fine model evaluations, or in terms of tolerances in arguments/function values; then, the space mapping algorithm to be used (checkboxes A, B, C, D, E and F as well as implicit SM panel at the bottom left corner of the interface); at last, the parameter extraction options (e.g., the number of responses used while matching the models), as well as constraints for

the coarse/fine model, regular SM parameters and implicit parameters. In our example, we only use term D (output SM) and implicit SM.

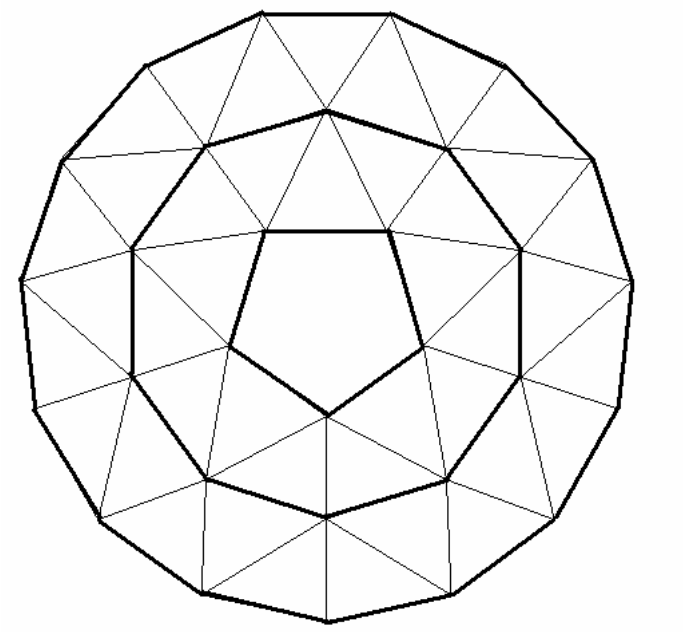

Fig. 5.3. Demonstration of local meshing of the annular ring in the coarse-mesh coarse model for a stacked probe-fed printed double ring antenna example.

TABLE 5.1

FINE MODEL AND COARSE MODEL IN DOUBLE ANNULAR RING ANTENNA

Model type	Technique	Meshing method	Mesh number	Frequency sweep time
Coarse model	Special Green's function + coarse mesh	Local meshing	83	8.721 seconds
Fine model	SEP	Global meshing density = 20	2661*	1 hour and 18 minutes*

* Number of meshes and time cost in the fine model are measured at the initial point.

Fig. 5.7 shows the setup of the FEKO driver (in our case both coarse and fine models are implemented in FEKO). The user has to provide the necessary information about the design variables, the FEKO input file as well as the type of response to be obtained from the model. This data will allow SMF to call the simulator for any required values of the design variables, acquire the simulation results, and prepare the model response in a required form.

Fig. 5.8 shows the setup for parameter extraction, surrogate optimization and trust region options.

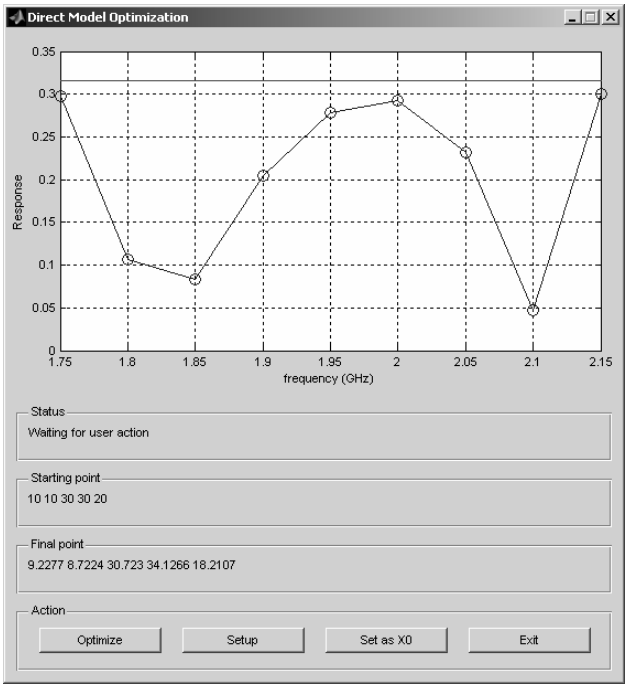

Fig. 5.4. Direct coarse model optimization interface in the SMF system.

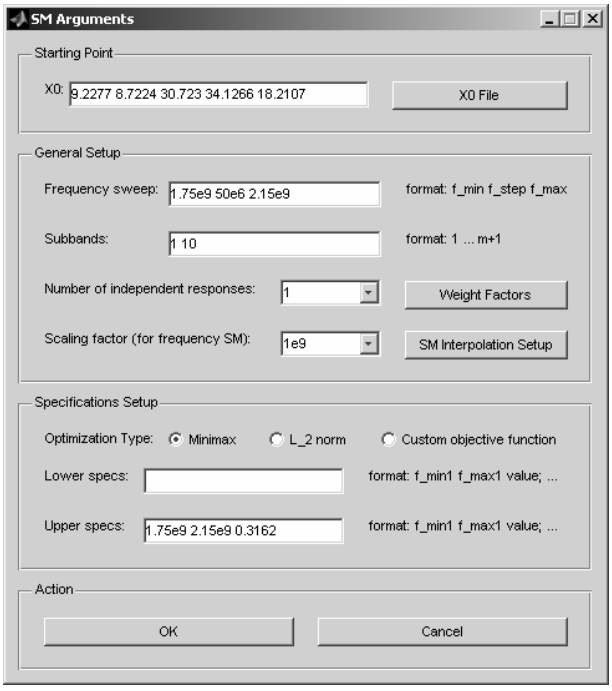

Fig. 5.5. SM arguments setup in the SMF system.

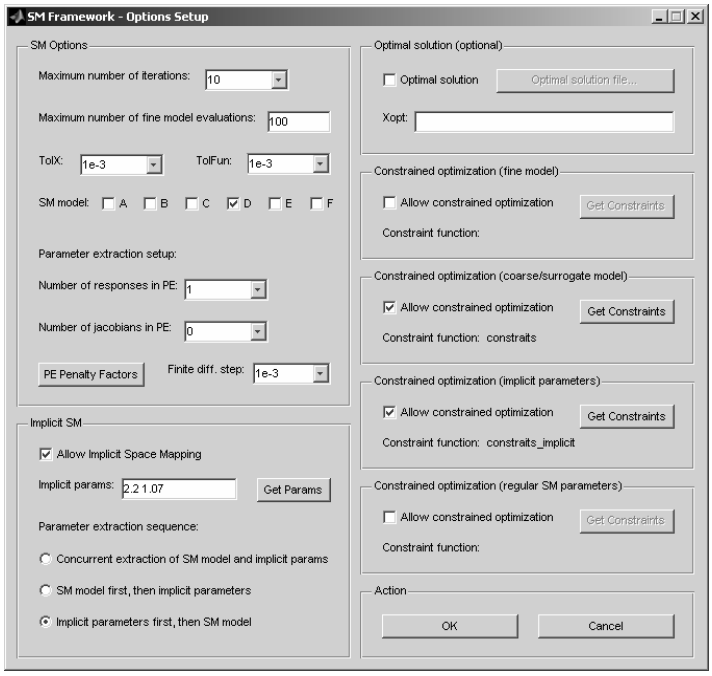

Fig. 5.6. Space mapping options setup in the SMF system.

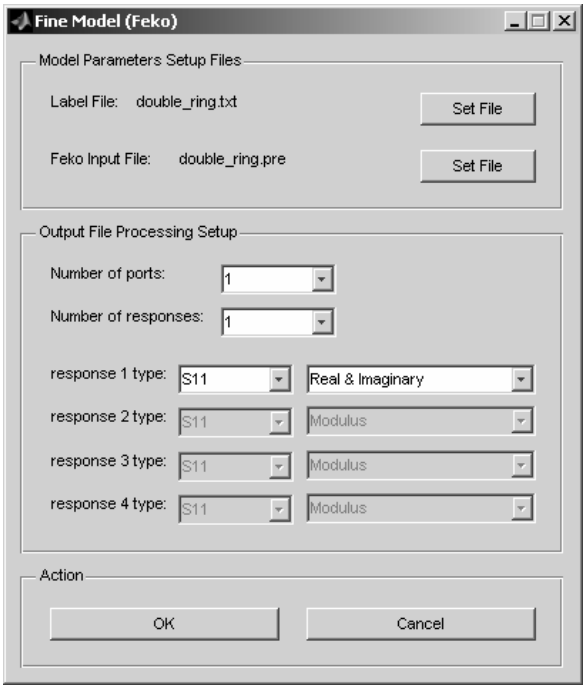

Fig. 5.7. FEKO driver setup in the SMF system.

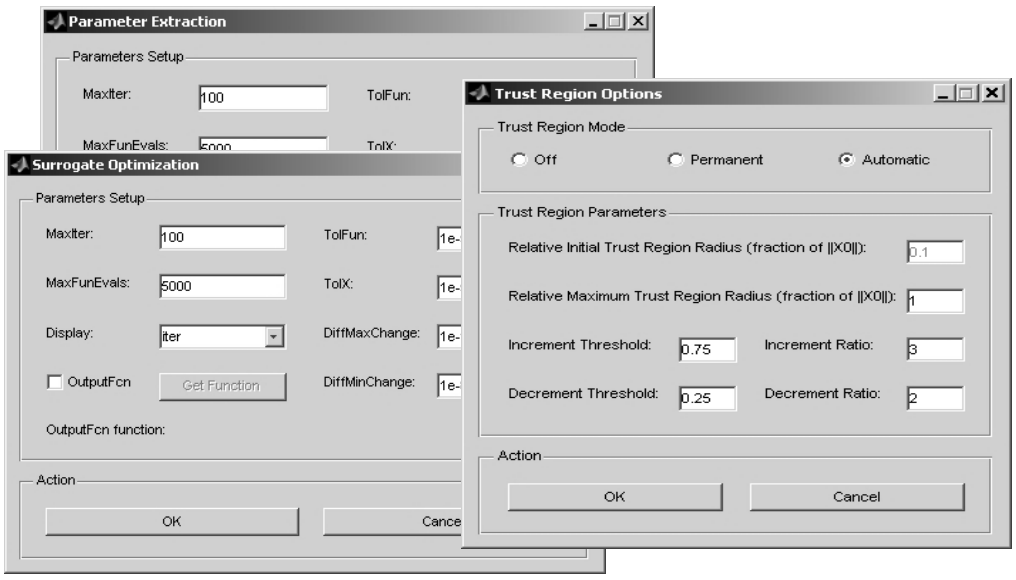

Fig. 5.8. Auxiliary setup in the SMF system: parameter extraction, surrogate optimization and trust region options.

SMF requires three iterations (four fine model simulations) to satisfy the specifications, although the coarse model initially exhibits a poor response (see Fig. 5.9). The total time taken is 5 hours 58 minutes (note that a single fine model simulation requires 1 hour 18 minutes). Fig. 5.10 depicts the fine and surrogate model responses at the final design. Good alignment is achieved through three PEs. Fig. 5.11 shows the reduction of the objective function versus the number of the iterations. Table 5.2 shows the initial and final design.

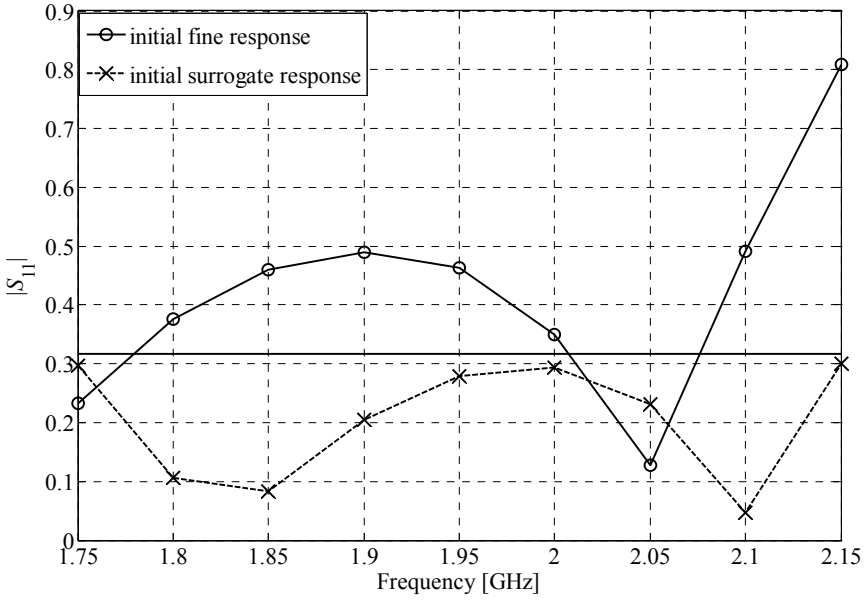

Fig. 5.9. Initial fine and surrogate responses corresponding to the coarse model optimal solution for the double annular ring antenna.

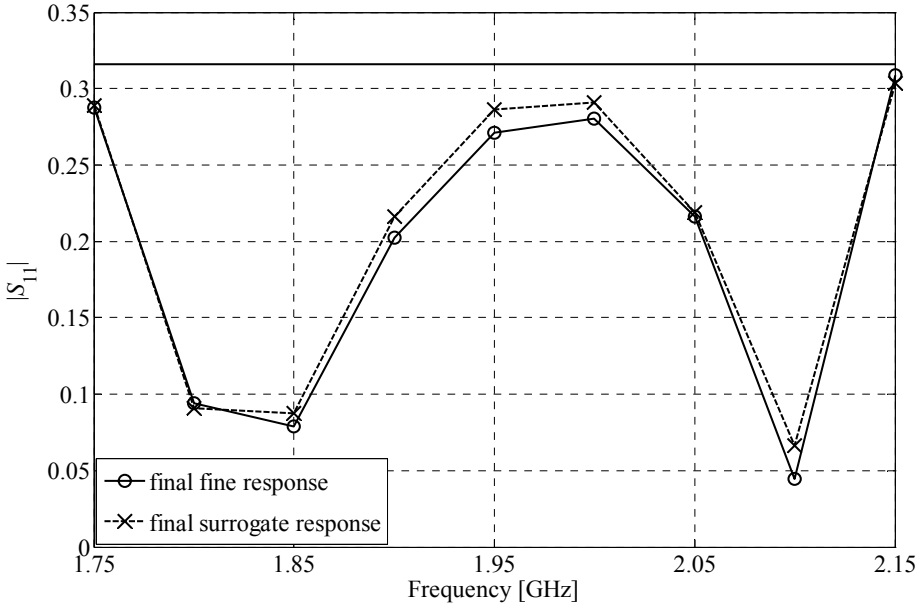

Fig. 5.10. Fine and surrogate responses for the double annular ring antenna example.

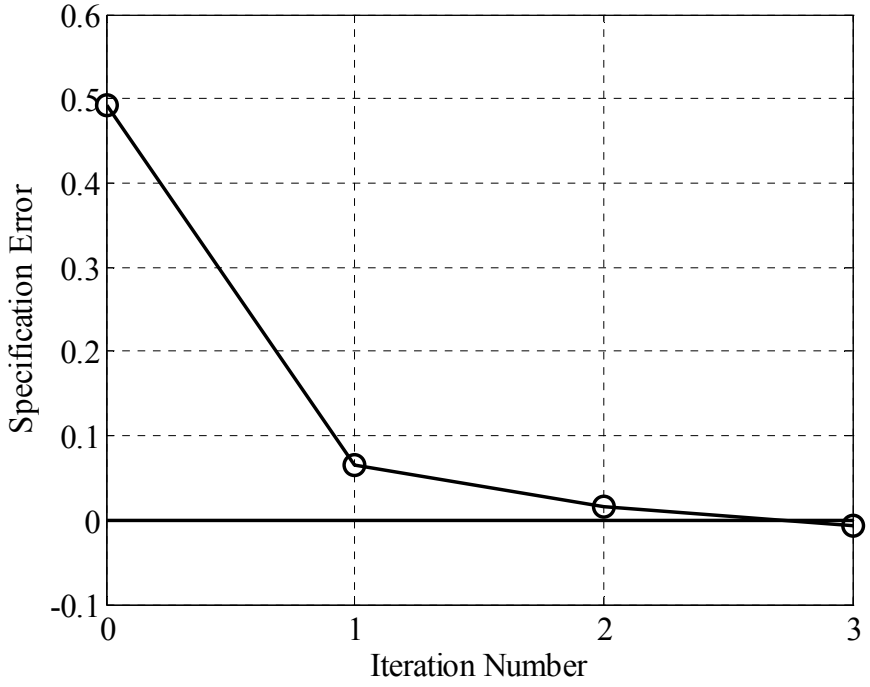

Fig. 5.11. Objective function value versus iteration number in the double annular ring antenna example.

TABLE 5.2

INITIAL AND FINAL DESIGN OF THE DOUBLE ANNULAR RING ANTENNA

Design parameters	Initial design (mm)	Final design (mm)
a_1	9.2277	10.6735
a_2	8.7224	7.8088
b_1	30.7230	28.4621
b_2	34.1266	32.5043
ρ_p	18.2107	19.6817

Fig. 5.12 shows the execution interface SMF, which was used to obtain the above results. Plots in the interface correspond to the algorithm status after the

last iteration. The top left plot shows the fine model response and design specifications; the top right plot shows the specification error vs. iteration number; the bottom left and bottom right plots are convergence plots that show $||\boldsymbol{x}^{(i+1)} - \boldsymbol{x}^{(i)}||$ and $||\boldsymbol{R}_f^{(i+1} - \boldsymbol{R}_f{}^{(i)}||$ vs. iteration number, respectively. The interface contains a number of controls including buttons to run/stop optimization, export graphs, create output files as well as browse through the previous iterations of the algorithm.

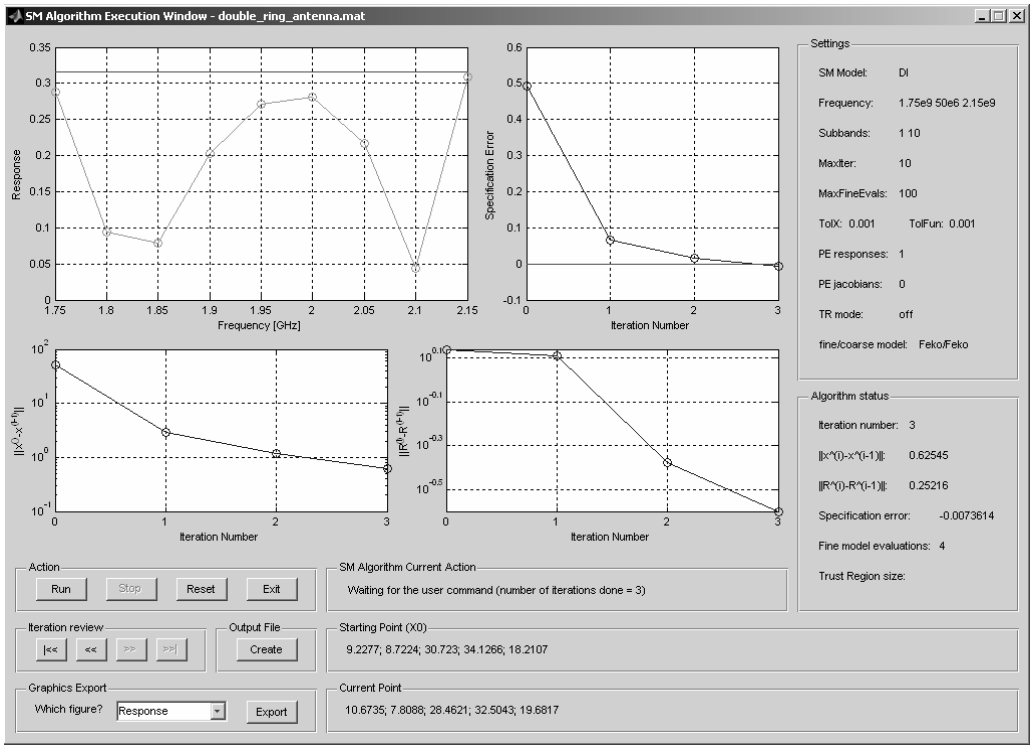

Fig. 5.12. Execution interface of SMF after the optimization procedure has stopped.

5.5.2 Patch Antenna

This patch antenna is printed on a substrate with relative dielectric constant $\varepsilon_r = 2.32$ and height $h = 1.59$ mm. The design parameters are the patch

length and width, i.e., $\boldsymbol{x}_f = [L\ W]^T$. The objective is to obtain $50\,\Omega$ input impedance at 2 GHz. The objective function is $|Z_{in} - 50|$.

In the fine model, the global mesh density is 30 meshes per wavelength. In the coarse model, the mesh number and topology are fixed through local meshing. We choose three mesh edges along L and seven along W. See Fig. 5.13. We use implicit SM and output SM. The selected preassigned SM parameter is $\boldsymbol{x} = \varepsilon_r$. In the PE, we match the complex S_{11} instead of the input impedance.

The initial design point is the coarse model optimal solution $\boldsymbol{x}_f^{(0)} = [47.1285\ \ 100.470]$ mm. SMF requires five iterations (six fine model simulations). Fig. 14 shows the reduction of the objective function versus the number of iterations. The final design is $\boldsymbol{x}_f^* = \boldsymbol{x}_f^{(4)} = [46.7294\ \ 99.6875]$ mm. Table 5.3 shows the optimization results for the design parameters, the objective function value, the preassigned parameter and the output SM parameter at each iteration. Computation time is 341 s, compared with 2816 s for direct fine model optimization. The SMF execution window is shown in Fig. 5.15.

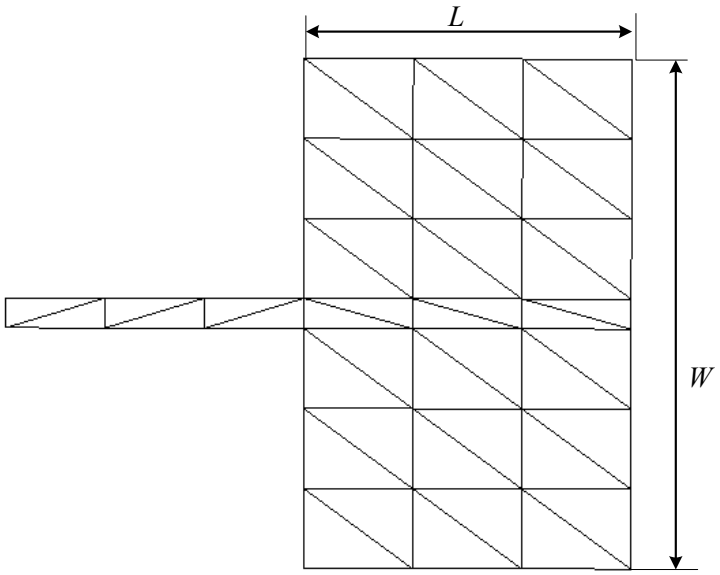

(a)

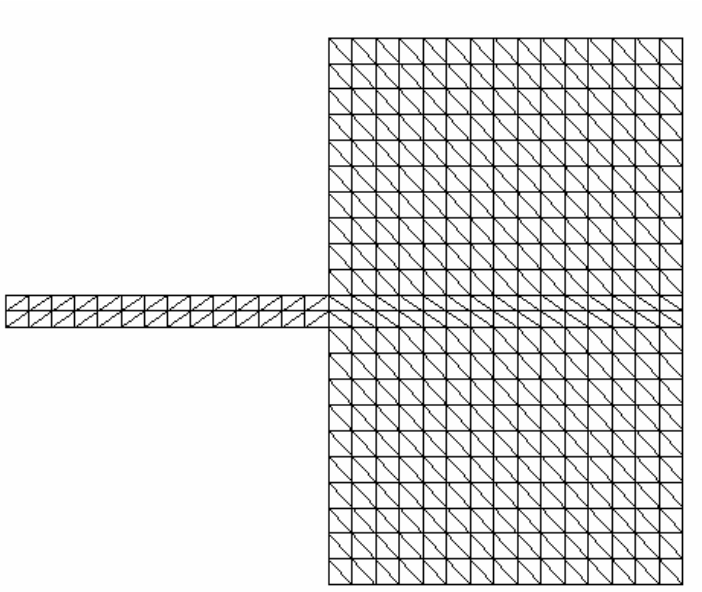

(b)

Fig. 5.13. Demonstration of the coarse model and the fine model. (a) The coarse model with three mesh edges along L and seven mesh edges along W. (b) The fine model with global mesh density of 30 meshes per wavelength.

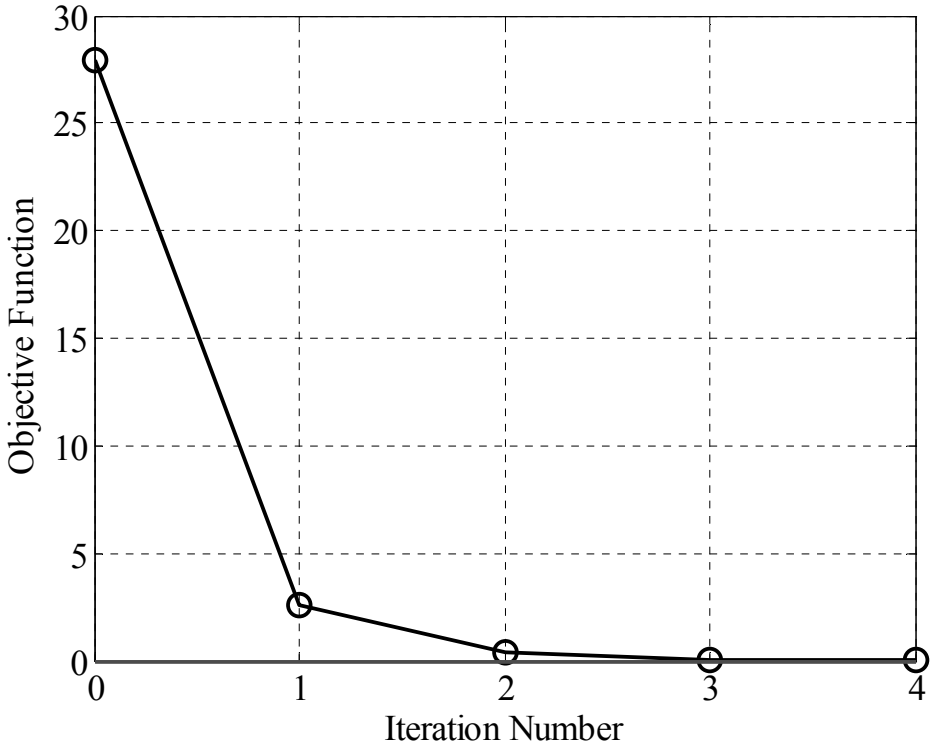

Fig. 5.14. Objective function value versus iteration number for the microstrip patch antenna example.

TABLE 5.3

OPTIMIZATION RESULTS FOR THE PATCH ANTENNA EXAMPLE

Iteration	$\boldsymbol{x}_f$ (mm)	ε_r	$\Delta \boldsymbol{R}$	$\lvert Z_{in} - 50 \rvert$
0	$\begin{bmatrix} 47.1285 \\ 100.470 \end{bmatrix}$	2.3200	0.0000	27.941
1	$\begin{bmatrix} 46.77743 \\ 99.6922 \end{bmatrix}$	2.3621	$0.0082 - 0.0461i$	2.5616
2	$\begin{bmatrix} 46.7268 \\ 99.6960 \end{bmatrix}$	2.3589	$0.0145 + 0.0056i$	0.35956
3	$\begin{bmatrix} 46.7294 \\ 99.6883 \end{bmatrix}$	2.3590	$0.0118 + 0.0054i$	2.4437×10^{-2}
4	$\begin{bmatrix} 46.7294 \\ 99.6875 \end{bmatrix}$	2.3589	$0.0115 + 0.0059i$	1.1234×10^{-2}

Instead of implicit SM and output SM (SM plan I), an alternative way to solve this problem involves input SM and output SM (SM plan II). To save time cost in the parameter extraction, we only choose the variable $\boldsymbol{c}$ in the input mapping (refer to Fig. 5.1 and (5.6)). The coarse model mesh discretization is the same (100 meshes). The algorithm takes 5 iterations and 695 s to reach the specification error 8.93×10^{-3}. The SM performance is shown in Fig. 5.16. As expected, it takes more time than the first SM option, because in the input SM, we

require two input SM variables in the parameter extraction rather than one as in the implicit SM.

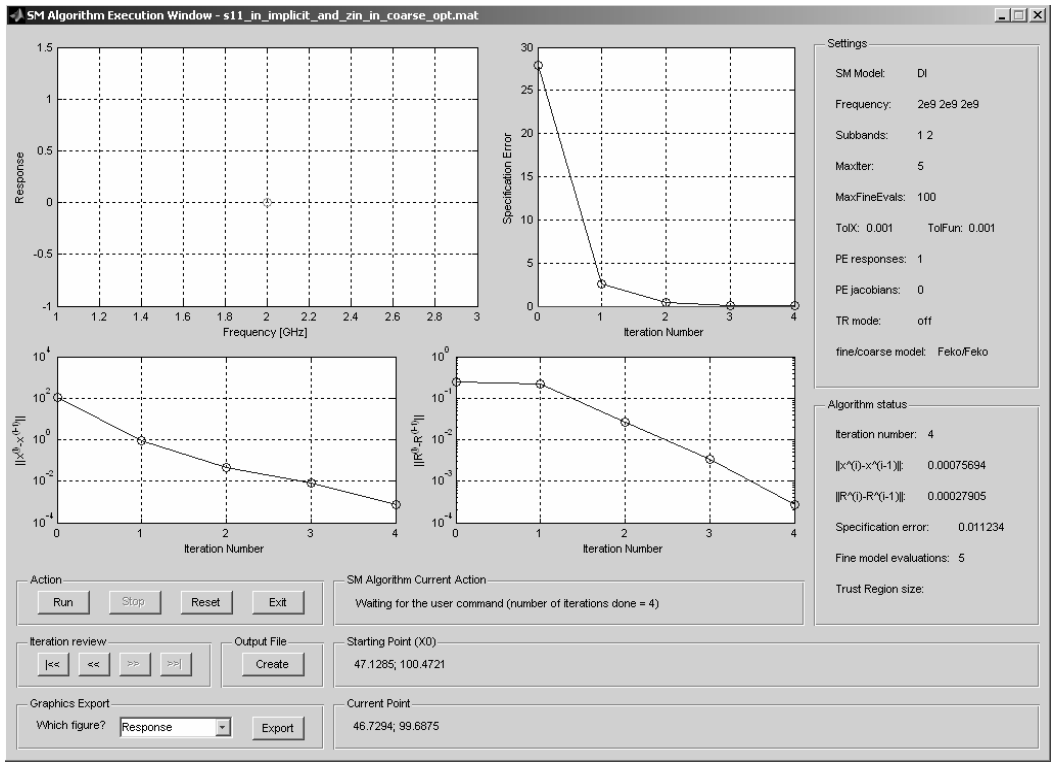

Fig. 5.15. The SMF system execution window for the patch antenna example (SM plan I: implicit SM and output SM).

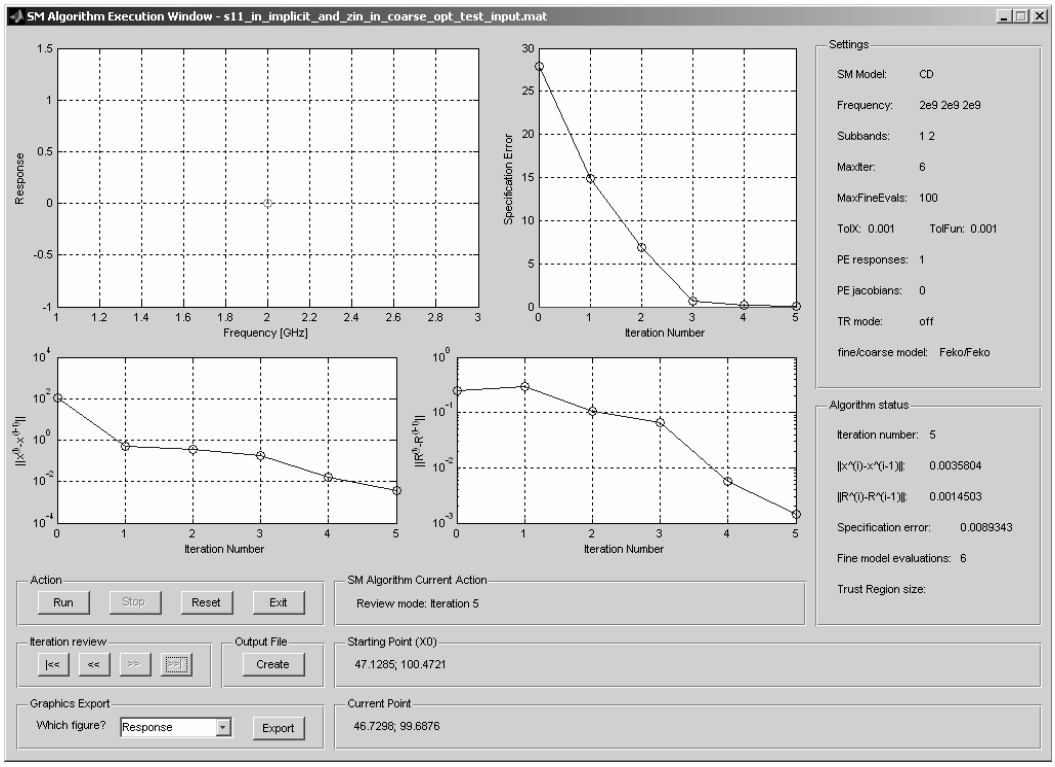

Fig. 5.16. The SMF execution window for the patch antenna example (SM plan II: input SM and output SM).

Table 5.4 discusses the effect on the SM performance of the coarseness of the coarse model for the patch antenna. The algorithm does not converge for 24 mesh elements (triangles). With an increase in the number of mesh elements, the function evaluation time increases while the SM iterations decrease. For SM plan I, we have the best SM performance in terms of total time cost for 100 mesh elements, which requires only 341 s. For SM plan II, we have the best SM for 48 mesh elements, which requires 479 s.

TABLE 5.4

THE EFFECT OF LOCAL MESHING ON SM PERFORMANCE

FOR THE PATCH ANTENNA

Local meshing in the coarse model				SM Plan I		SM Plan II	
Mesh number along		Total mesh number	Function evaluation time (s)	Iteration number	Total time (s)	Iteration number	Total time (s)
L	W						
2	5	24	0.109	Not convergent		Not convergent	
3	7	48	0.219	6	364	9	479
5	9	100	0.438	4	341	5	695
9	20	400	4.063	4	1604	3	2659
11	22	528	8.375	3	2695	3	3220
Global meshing in the fine model				Direct optimization			
Mesh density=30		1032*	33.313*	2816 s			

* The number of meshes and function evaluation time for the fine model is measured at the starting point $[L\ W] = [55\ 85]$ mm

5.6 CONCLUDING REMARKS

We have presented an effective space-mapping technique for antenna optimization based on a coarse model, which exploits a coarse non-convergent mesh of fixed topology. Both coarse and fine models are implemented by the same MoM solver. A separate coarse model is not required. In the double annular ring example, the SMF system provides an efficient way to address the finite

ground size problem. We solve the optimal impedance of a patch antenna problem using two SM plans. The coarseness in the coarse model and its effect on the space mapping performance are discussed. Although we demonstrate our approach through antenna design, it is applicable to other planar structures.

REFERENCES

[1] J.W. Bandler, R.M. Bienacki, S.H. Chen, P.A. Grobelny and R.H. Hemmers, "Space mapping technique for electromagnetic optimization," *IEEE Trans. Microwave Theory Tech*., vol. 42, Dec. 1994, pp. 2536-2544.

[2] J.W. Bandler, Q.S. Cheng, N.K. Nikolova and M. A. Ismail, "Implicit space mapping optimization exploiting preassigned parameters," *IEEE Trans. Microwave Theory Tech.*, vol. 52, Jan. 2004, pp. 378-385.

[3] J.W. Bandler, Q.S. Cheng, D. Gebre-Mariam, K. Madsen, F. Pedersen and J. Søndergaard, "EM-based surrogate modeling and design exploiting implicit, frequency and output space mappings," in *IEEE MTT-S IMS Dig.*, June. 2003, pp.1003-1006.

[4] M.H. Bakr, J.W. Bandler, M.A. Ismail, J.E. Rayas-Sánchez and Q.J. Zhang, "Neural space-mapping optimization for EM-based design," *IEEE Trans. Microwave Theory Tech.*, vol. 48, Dec. 2000, pp. 2307-2315.

[5] M.A. Ismail, D. Smith, A. Panariello, Y. Wang and M. Yu, "EM-based design of large-scale dielectric-resonator filters and multiplexers by space mapping," *IEEE Trans. Microwave Theory Tech*., vol. 52, Jan. 2004, pp. 386-392.

[6] K.-L. Wu, Y.-J. Zhao, J. Wang, and M.K.K Cheng, "An effective dynamic coarse model for optimization design of LTCC RF circuits with aggressive space mapping," *IEEE Trans. Microwave Theory Tech*., vol. 52, Jan. 2004, pp. 393-402.

[7] J. Zhu, J.W. Bandler, N.K. Nikolova and S. Koziel, "Antenna design through space mapping optimization," *IEEE MTT-S Int. Microwave Symp.*, San Francisco, California, 2006.

[8] J. Zhu, J.W. Bandler, N.K. Nikolova and S. Koziel, "Antenna optimization through space mapping," submitted to *IEEE Trans. Antennas Propagat., Special Issue on Synthesis and Optimization Techniques in Electromagnetics and Antenna System Design*, Jan. 2007.

[9] FEKO® *User's Manual*, Suite 4.2, June 2004, EM Software & Systems-S.A. (Pty) Ltd, 32 Techno Lane, Technopark, Stellenbosch, 7600, South Africa, http://www.feko.info. In the USA: EM Software & Systems (USA), Inc., 24 Research Drive, Hampton, VA 23666, USA, http://www.emssusa.com/.

[10] J.W. Bandler, A.S. Mohamed and M.H. Bakr, "TLM-based modeling and design exploiting space mapping," *IEEE Trans. Microwave Theory Tech*., vol. 53, Sep. 2005, pp. 2801-2811.

[11] SMF, Bandler Corporation, P.O. Box 8083, Dundas, ON, Canada L9H 5E7, 2006.

[12] "Mesh refinement," *FEKO Quarterly*, December 2004.

[13] S. Koziel, J.W. Bandler and K. Madsen, "Towards a rigorous formulation of the space mapping technique for engineering design," *Proc. ISCAS, Kobe,* Japan, Jun. 2005, pp. 5605-5608.

[14] D.M. Kotokoff, J.T. Aberle and R.B. Waterhouse, "Rigorous analysis of probe-fed printed annular ring antennas," *IEEE Trans. Antennas Propagat,* vol. 47, Feb. 1999, pp. 384-388.

[15] F. Tavakkol-Hamedani, L. Shafai and G.Z. Rafi, "The effects of substrate and ground plane size on the performance of finite rectangular microstrip antennas," *IEEE AP-S/URSI Int. Symp. on Antennas Propagat.*, Jun. 2002.

[16] A.K. Bhattacharyya, "Effects of ground plane truncation on the impedance of a patch antenna," *IEE proceedings-H*, vol. 138, Dec. 1991, pp. 560-564.

[17] "Modeling of dielectric materials in FEKO," *FEKO Quarterly*, March 2005.

CHAPTER 5 ANTENNA DESIGN THROUGH SPACE MAPPING OPTMIZATION

PART III

CONCLUSIONS

CONCLUSIONS

The thesis presents novel methods for the computer-aided design of microwave circuits and antennas exploiting adjoint-variable and space mapping (SM) technologies. These technologies are demonstrated by various examples.

In Chapter 2, some relevant features of the method of moments (MoM) are reviewed. These features are related to further developments in this thesis, especially the developments of the self-adjoint sensitivity analysis and the coarse-mesh surrogate model optimization technique. After a brief introduction to the MoM, the CPU time cost versus mesh density is discussed, followed by mesh refinement and mesh convergence. A discussion on the modeling of dielectric objects with the MoM is also given.

In Part I (Chapters 3 and 4), we investigate the sensitivity analysis in the frequency domain. In Chapter 3, we propose the self-adjoint sensitivity analysis (SASA) method for network parameter sensitivity calculation in the MoM. It reduces the computational cost of the AVM by avoiding the adjoint analysis. Since the derivative of system matrix is obtained using finite differences, this technique is also referred to as finite-difference self-adjoint sensitivity analysis (FD-SASA). We propose a general procedure to implement the FD-SASA technique and demonstrate how it works with the commercial solver FEKO. The MoM matrix symmetry versus the convergence of the solution and the computational overhead associated with the sensitivity analysis are rigorously discussed at the end of this chapter.

In Chapter 4, the EM optimization using sensitivity analysis in the frequency domain is studied. The Broyden update is utilized in the iterative computation of the system matrix derivatives, which are then used in the self-adjoint formula to obtain the response Jacobian. This SASA method is referred to as B-SASA. It significantly reduces the computational overhead compared with the FD-SASA proposed in Chapter 3. Two criteria are used to switch back and forth throughout the optimization process between the robust but more time-demanding FD-SASA and the B-SASA. Thus, we avoid the inaccuracy, which may accumulate in the B-SASA method, while in the same time fully exploit its computational efficiency. This hybrid approach (B/FD-SASA) guarantees good accuracy of the gradient information with minimal computational time.

Chapter 5 in Part II presents the antenna design optimization exploiting space mapping techniques. We exploit a coarse-mesh MoM solver as the coarse model and align it with the fine-mesh MoM solution through space mapping. Two space mapping plans are employed: (1) implicit space mapping and output space mapping, (2) input space mapping and output space mapping. A novel local meshing method avoids inconsistencies in the coarse model. The proposed plans are implemented through SMF. Our approach is illustrated with the MoM-based design of a double annular ring antenna and a patch antenna. The SMF algorithms converge to a good design in spite of the poor initial behavior of the coarse-mesh MoM surrogate.

CONCLUSIONS

The Appendix shows the calculation of the *S*-parameters from the current solution of the MoM. It is needed in Chapter 3 in order to derive the *S*-parameter self-adjoint sensitivity analysis formulas.

The following research topics should be addressed in future developments.

(1) Exploiting the self-adjoint sensitivity analysis technique for the gradient-based SM optimization and modeling.

(2) Investigating the multi-level MoM and model order reduction (MOR) techniques to build robust surrogate models.

(3) Investigating further the properties of the coarse-mesh coarse models in MoM simulations. Focus should be on robust criteria to evaluate the suitability of the coarse models.

APPENDIX

NETWORK PARAMETER CALCULATION IN FEKO

In this section, we show how to calculate the two-port *S*-parameters based on the solution (current vector) available from FEKO.

According to the network theory,

$$\begin{bmatrix} U_1 \\ U_2 \end{bmatrix} = \begin{bmatrix} Z_{11} & Z_{12} \\ Z_{21} & Z_{22} \end{bmatrix} \cdot \begin{bmatrix} I_1 \\ I_2 \end{bmatrix} \tag{A.1}$$

When Port 1 is excited,

$$V_1 - Z_0 I_{11} = Z_{11} I_{11} + Z_{12} I_{21} \tag{A.2}$$

$$-Z_0 I_{21} = Z_{21} I_{11} + Z_{22} I_{21} \tag{A.3}$$

when Port 2 is excited,

$$V_2 - Z_0 I_{22} = Z_{21} I_{12} + Z_{22} I_{22} \tag{A.4}$$

$$-Z_0 I_{12} = Z_{11} I_{12} + Z_{12} I_{22} \tag{A.5}$$

Here, I_{PQ} represents the induced current at port P due to the excitation at port Q. $P, Q = 1, 2$. They can be obtained from FEKO.

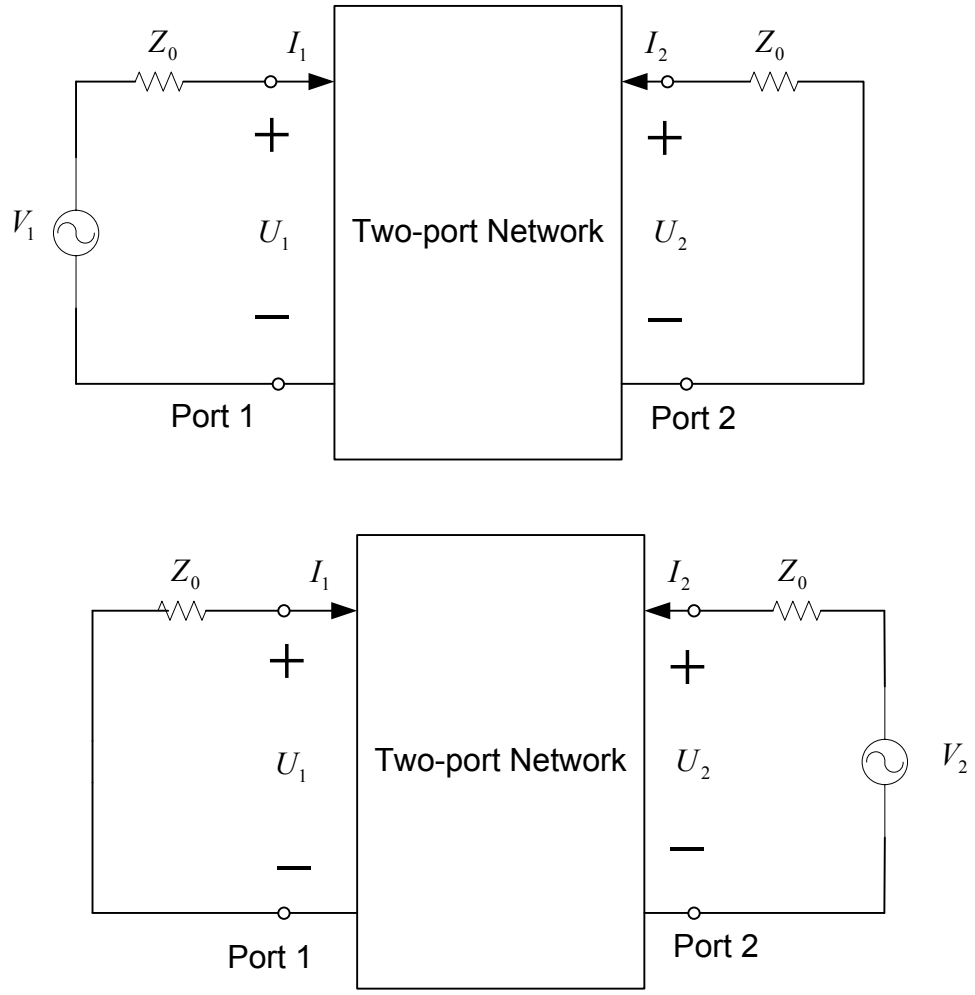

Fig.A.1. Demonstration of a two-port network.

From equations (A.2) - (A.5), we obtain:

$$Z_{11} = -Z_0 - \frac{V_1 I_{22}}{I_{12} I_{21} - I_{11} I_{22}} \tag{A.6}$$

$$Z_{12} = \frac{V_1 I_{12}}{I_{12} I_{21} - I_{11} I_{22}} \tag{A.7}$$

$$Z_{21} = \frac{V_2 I_{21}}{I_{12} I_{21} - I_{11} I_{22}} \tag{A.8}$$

$$Z_{22} = -Z_0 - \frac{V_2 I_{11}}{I_{12} I_{21} - I_{11} I_{22}} \tag{A.9}$$

We use the relationship between the *Z*- and the *S*-parameters as

$$\Delta Z = (Z_{11} + Z_0)(Z_{22} + Z_0) - Z_{12} Z_{21} = \frac{V_1 V_2}{I_{11} I_{22} - I_{12} I_{21}} \tag{A.10}$$

$$\begin{aligned} S_{11} &= \frac{(Z_{11} - Z_0)(Z_{22} + Z_0) - Z_{12} Z_{21}}{\Delta Z} \\ &= \frac{(2Z_0 + \frac{V_1 I_{22}}{I_{12} I_{21} - I_{11} I_{22}}) \cdot \frac{V_2 I_{11}}{I_{12} I_{21} - I_{11} I_{22}} - \frac{V_1 I_{12}}{I_{12} I_{21} - I_{11} I_{22}} \cdot \frac{V_2 I_{21}}{I_{12} I_{21} - I_{11} I_{22}}}{\frac{V_1 V_2}{I_{11} I_{22} - I_{12} I_{21}}} \\ &= -\frac{2Z_0 I_{11}}{V_1} + 1 \end{aligned} \tag{A.11}$$

$$S_{12} = \frac{2Z_{12}Z_0}{\Delta Z} = \frac{\dfrac{2Z_0 V_1 I_{12}}{I_{12}I_{21} - I_{11}I_{22}}}{\dfrac{V_1 V_2}{I_{11}I_{22} - I_{12}I_{21}}} = \frac{-2Z_0 I_{12}}{V_2} \tag{A.12}$$

$$S_{21} = \frac{2Z_{21}Z_0}{\Delta Z} = \frac{\dfrac{2Z_0 V_2 I_{21}}{I_{12}I_{21} - I_{11}I_{22}}}{\dfrac{V_1 V_2}{I_{11}I_{22} - I_{12}I_{21}}} = \frac{-2Z_0 I_{21}}{V_1} \tag{A.13}$$

$$\begin{aligned} S_{22} &= \frac{(Z_{11} + Z_0)(Z_{22} - Z_0) - Z_{12}Z_{21}}{\Delta Z} \\ &= \frac{\dfrac{V_1 I_{22}}{I_{12}I_{21} - I_{11}I_{22}} \cdot (2Z_0 + \dfrac{V_2 I_{11}}{I_{12}I_{21} - I_{11}I_{22}}) - \dfrac{V_1 I_{12}}{I_{12}I_{21} - I_{11}I_{22}} \cdot \dfrac{V_2 I_{21}}{I_{12}I_{21} - I_{11}I_{22}}}{\dfrac{V_1 V_2}{I_{11}I_{22} - I_{12}I_{21}}} \\ &= -\frac{2Z_0 I_{22}}{V_2} + 1 \end{aligned} \tag{A.14}$$

For *N*-port *S*-parameter calculation, we can obtain a more general expression in the same way:

$$S_{PQ} = \begin{cases} \dfrac{-2Z_0 I_{PQ}}{V_Q} + 1, & \text{when } P = Q \\ \dfrac{-2Z_0 I_{PQ}}{V_Q}, & \text{when } P \neq Q \end{cases} \tag{A.15}$$

BIBLIOGRAPHY

Advanced Design System 2003C, *User's Manual*, Agilent Technologies, 395 Page Mill Road, Palo Alto, CA 94304, USA.

Agilent ADS, Agilent Technologies, 1400 Fountaingrove Parkway, Santa Rosa, CA 95403-1799, USA.

H. Akel and J.P. Webb, "Design sensitivities for scattering-matrix calculation with tetrahedral edge elements," *IEEE Trans. Magnetics*, vol. 36, July 2000, pp. 1043-1046.

S.M. Ali, N.K. Nikolova and M.H. Bakr, "Recent advances in sensitivity analysis with frequency-domain full-wave EM solvers," *Applied Computational Electromagnetics Society Journal*, vol. 19, Nov. 2004, pp. 147-154.

S. Amari, "Numerical cost of gradient computation within the method of moments and its reduction by means of a novel boundary-layer concept," *IEEE MTT-S Int. Microwave Symp*. *Digest*, 2001, pp.1945-1948.

Ansoft HFSS, Ansoft Corporation, 225 West Station Square Drive, Suite 200, Pittsburgh, PA 15219, USA.

M.H. Bakr, *Advances in Space Mapping Optimization of Microwave Circuits*, PhD Thesis, Department of Electrical and Computer Engineering, McMaster University, 2000.

M.H. Bakr, J.W. Bandler and N. Georgieva, "An aggressive approach to parameter extraction," *IEEE Trans. Microwave Theory Tech*., vol. 47, Dec. 1999, pp. 2428-2439.

M.H. Bakr, J.W. Bandler, M.A. Ismail, J.E. Rayas-Sánchez and Q.J. Zhang, "Neural space-mapping optimization for EM-based design," *IEEE Trans. Microwave Theory Tech.*, vol. 48, Dec. 2000, pp. 2307-2315.

M.H. Bakr, J.W. Bandler, K. Madsen and J. Søndergaard, "An introduction to the space mapping technique," *Optimization Eng*., vol. 2, 2001, pp.369-384.

M.H. Bakr and N.K. Nikolova, "An adjoint variable method for frequency domain TLM problems with conducting boundaries," *IEEE Microwave and Wireless Components Letters,* vol. 13, Sep. 2003, pp. 408-410.

C.A. Balanis, *Antenna Theory: Analysis and Design*, New York: Wiley, 1997.

J.W. Bandler, R.M. Biernacki and S.H. Chen, "Fully automated space mapping optimization of 3D structures," in *IEEE MTT-S Int. Microwave Symp. Dig.*, San Francisco, CA, 1996, pp. 753-756.

J.W. Bandler, R.M. Biernacki, S.H. Chen, W.J. Getsinger, P.A. Grobelny, C. Moskowitz and S.H. Talisa, "Electromagnetic design of high temperature superconducting microwave filters," *Int. J. RF Microwave Computer-Aided Eng.*, vol. 5, 1995, pp. 331-343.

J.W. Bandler, R.M. Biernacki, S.H. Chen, P.A. Grobelny and R.H. Hemmers, "Space mapping technique for electromagnetic optimization," *IEEE Trans. Microwave Theory Tech*., vol. 42, 1994, pp. 2536-2544.

J.W. Bandler, R.M. Biernacki, S.H. Chen and Y.F. Huang, "Design optimization of interdigital filters using aggressive space mapping and decomposition," *IEEE Trans. Microwave Theory Tech*., vol. 45, May 1997, pp. 761-769.

J.W. Bandler, R.M. Biernacki, S.H. Chen and D. Omeragic, "Space mapping optimization of waveguide filters using finite element and mode-matching electromagnetic simulators," *Int. J. RF Microwave Computer-Aided Eng.,* vol. 9, 1999, pp. 54-70.

J.W. Bandler, S.H. Chen, S. Daijavad and K. Madsen, "Efficient optimization with integrated gradient approximations," *IEEE Trans. Microwave Theory Tech*., vol. 36, Feb. 1988, pp. 444-455.

J.W. Bandler, Q.S. Cheng, S.A. Dakroury, A.S. Mohamed, M.H. Bakr, K. Madsen and J. Søndergaard, "Trends in space mapping technology for engineering optimization," *3rd Annual McMaster Optimization Conference: Theory and Applications*, *MOPTA03*, Hamilton, ON, Aug. 2003.

J.W. Bandler, Q. Cheng, S.A. Dakroury, A.S. Mohamed, M.H. Bakr, K. Madsen and J. Søndergaard, "Space mapping: the state of the art," in *SBMO/MTT-S*

International Microwave and Optoelectronics Conference (*IMOC 2003*), Parana, Brazil, Sep. 2003, vol. 2, pp. 951-956.

J.W. Bandler, Q. Cheng, S.A. Dakroury, A.S. Mohamed, M.H. Bakr, K. Madsen and J. Søndergaard, "Space mapping: the state of the art," *IEEE Trans. Microwave Theory and Tech*., vol. 52, Jan. 2004, pp. 337-361.

J.W. Bandler, Q.S. Cheng, D. Gebre-Mariam, K. Madsen, F. Pedersen and J. Søndergaard, "EM-based surrogate modeling and design exploiting implicit, frequency and output space mappings," in *IEEE MTT-S Int. Microwave Symp. Dig.,* Philadelphia, PA, 2003, pp. 1003-1006.

J.W. Bandler, Q.S. Cheng, D.M. Hailu, A.S. Mohamed, M.H. Bakr, K. Madsen and F. Pedersen, "Recent trends in space mapping technology," in *Proc. 2004 Asia-Pacific Microwave Conf. APMC04*, New Delhi, India, Dec. 2004.

J.W. Bandler, Q.S. Cheng and S. Koziel, "Implementable space mapping approach to enhancement of microwave device models," *IEEE MTT-S Int. Microwave Symp. Dig*. (Long Beach, CA, June 2005) pp. 1139-1142.

J.W. Bandler, Q.S. Cheng, N.K. Nikolova and M.A. Ismail, "Implicit space mapping optimization exploiting preassigned parameters," *IEEE Trans. Microw. Theory Tech*., vol. 52, Jan. 2004, pp. 378-385.

J.W. Bandler, D.M. Hailu, K. Madsen and F. Pedersen, "A space-mapping interpolating surrogate algorithm for highly optimized EM-based design of microwave devices," *IEEE Trans. Microwave Theory and Tech*., vol. 52, Nov. 2004, pp. 2593-2600.

J.W. Bandler, M.A. Ismail and J.E. Rayas-Sánchez, "Expanded space mapping EM-based design framework exploiting preassigned parameters," *IEEE Trans. Circuits Syst.-I*, vol. 49, Dec. 2002, pp. 1833-1838.

J.W. Bandler, W. Kellerman and K. Madsen, "A superlinearly convergent minimax algorithm for microwave circuit design," *IEEE Trans. Microwave Theory Tech.*, vol. MTT-33, Dec. 1985, pp. 1519-1530.

J.W. Bandler, A.S. Mohamed and M.H. Bakr, "TLM-based modeling and design exploiting space mapping," *IEEE Trans. Microwave Theory Tech*., vol. 53, 2005, pp. 2801-2811.

J. W. Bandler, A. S. Mohamed, M. H. Bakr, K. Madsen and J. Søndergaard, "EM-based optimization exploiting partial space mapping and exact sensitivities," *IEEE Trans. Microwave Theory Tech*., vol. 50, Dec. 2002, pp. 2741-2750.

A.D Belegundu and T.R. Chandrupatla, *Optimization Concepts and Applications in Engineering.* Upper Saddle River, NJ: Prentice-Hall, 1999.

A. K. Bhattacharyya, "Effects of ground plane truncation on the impedance of a patch antenna," *IEE proceedings-H*, vol. 138, Dec. 1991, pp. 560-564.

R.M. Biernacki, J.W. Bandler, J. Song and Q.J. Zhang, "Efficient quadratic approximation for statistical design," *IEEE Trans. Circuits Syst*., vol. 36, Nov. 1989, pp. 1449-1454.

C.G. Broyden, "A class of methods for solving nonlinear simultaneous equations," *Mathematics of Computation*, vol. 19, 1965, pp. 577-593.

D.G. Cacuci, *Sensitivity & Uncertainty Analysis, Volume 1: Theory.* Boca Raton, FL: Chapman & Hall/CRC, 2003.

Q. Cheng, *Advances in Space Mapping Technology Exploiting Implicit Space Mapping and Output Space Mapping*, PhD Thesis, Department of Electrical and Computer Engineering, McMaster University, 2004.

Y.S. Chung, C. Cheon, I.H. Park and S.Y. Hahn, "Optimal design method for microwave device using time domain method and design sensitivity analysis—part I: FETD case," *IEEE Trans. Magnetics*, vol. 37, Sep. 2001, pp. 3289-3293.

L. Daniel, *Simulation and Modeling Techniques for Signal Integrity and Electromagnetic Interference on High Frequency Electronic Systems*, PhD thesis, Electrical Engineering and Computer Science, University of California at Berkeley.

em, Sonnet Software, Inc. 100 Elwood Davis Road, North Syracuse, NY 13212, USA.

FEKO® User's Manual, Suite 4.2, June 2004, EM Software & Systems-S.A. (Pty) Ltd, 32 Techno Lane, Technopark, Stellenbosch, 7600, South Africa, http://www.feko.info. In the USA: EM Software & Systems (USA), Inc., 24 Research Drive, Hampton, VA 23666, USA, http://www.emssusa.com/.

M.D. Greenberg, *Advanced Engineering Mathematics*. Upper Saddle River, N.J.: Prentice Hall, 1998, pp. 1138-1140.

N.K. Georgieva, S. Glavic, M.H. Bakr and J.W. Bandler, "Feasible adjoint sensitivity technique for EM design optimization," *IEEE Trans. Microwave Theory Tech.,* vol. 50, Dec. 2002, pp. 2751-2758.

P.A. Grobelny, *Integrated Numerical Modeling Techniques for Nominaland Statistical Circuit Design*, Ph.D. Thesis, Department of Electrical and Computer Engineering, McMaster University, Hamilton, ON, Canada,1995.

E.J. Haug, K.K. Choi and V. Komkov, *Design Sensitivity Analysis of Structural Systems*. Orlando, FL: Academic, 1986.

R.F. Harrington, *Field Computation by Moment Methods*, New York, NY: Macmillan, 1968.

M.A. Ismail, D. Smith, A. Panariello, Y. Wang and M. Yu, "EM-based design of large-scale dielectric-resonator filters and multiplexers by space mapping," *IEEE Trans. Microwave Theory Tech*., vol. 52, Jan. 2004, pp. 386-392.

U. Jakobus, "Comparison of different techniques for the treatment of lossy dielectric/magnetic bodies within the method of moments formulation," *AEÜ International Journal of Electronics and Communications*, vol. 54, 2000, pp. 163-173.

D. M. Kotokoff, J. T. Aberle and R. B. Waterhouse, "Rigorous analysis of probe-fed printed annular ring antennas," *IEEE Trans. Antennas Propagat*, vol. 47, Feb. 1999, pp. 384-388.

S. Koziel, J.W. Bandler and K. Madsen, "Towards a rigorous formulation of the space mapping technique for engineering design," *Proc. ISCAS, Kobe*, Japan, June. 2005, pp. 5605-5608.

S. Koziel, J.W. Bandler, A.S. Mohamed and K. Madsen "Enhanced surrogate models for statistical design exploiting space mapping technology," *IEEE MTT–S Int. Microwave Symp. Dig*. (Long Beach, CA, June 2005) pp.1609-1612.

Hong-bae Lee and T. Itoh, "A systematic optimum design of waveguide-to-microstrip transition," *IEEE Trans. Microwave Theory Tech*., vol. 45, May 1997, pp. 803-809.

D. Li and N. K. Nikolova, "S-parameter sensitivity analysis of waveguide structures with FEMLAB," *COMSOL Multiphysics Conf.*, Cambridge, MA, Oct. 2005, pp. 267-271.

D. Li, J. Zhu, N.K. Nikolova, M.H. Bakr and J.W. Bandler, "EM optimization using sensitivity analysis in the frequency domain," submitted to *IEEE Trans. Antennas Propagat., Special Issue on Synthesis and Optimization Techniques in Electromagnetics and Antenna System Design*, Jan. 2007.

MEFiSTo-3D, Faustus Scientific Corporation, 1256 Beach Drive, Victoria, BC, V8S 2N3, Canada.

"Mesh refinement," *FEKO Quarterly*, December 2004.

"Modelling of dielectric materials in FEKO," *FEKO Quarterly*, Mar. 2005.

A.S. Mohamed, *Recent Trends in CAD Tools for Microwave Circuit Design Exploiting Space Mapping Technology*, PhD Thesis, Department of Electrical and Computer Engineering, McMaster University, 2005.

N.K. Nikolova, J.W. Bandler and M.H. Bakr, "Adjoint techniques for sensitivity analysis in high-frequency structure CAD," *IEEE Trans. Microwave Theory Tech*., vol. 52, Jan. 2004, pp. 403-419.

P. Neittaanmäki, M. Rudnicki and A. Savini, *Inverse Problems and Optimal Design in Electricity and Magnetism*. New York: Oxford University Press, 1996, Chapter 4.

N.K Nikolova, R. Safian, E.A. Soliman, M.H. Bakr and J.W. Bandler, "Accelerated gradient based optimization using adjoint sensitivities," *IEEE Trans. Antenna Propagat*. vol. 52, Aug. 2004, pp. 2147-2157.

N.K. Nikolova, J. Zhu, D. Li and M.H. Bakr, "Extracting the derivatives of network parameters from frequency-domain electromagnetic solutions," the *XXVIIIth General Assembly of the International Union of Radio Science*, CDROM, Oct. 2005.

N.K. Nikolova, J. Zhu, D. Li, M.H. Bakr and J.W. Bandler, "Sensitivity analysis of network parameters with electromagnetic frequency-domain simulators," *IEEE Trans. Microwave Theory Tech*., vol. 54, Feb. 2006, pp. 670-681.

D. M. Pozar, *Microwave Engineering, 2nd ed*., New York: John Wiley & Sons, 1998, Chapter 4.

I.D. Robertson and S. Lucyszyn, *RFIC and MMIC design and technology*, *IEE Circuits, Device and System*, Series 13, 2001.

R. Safian, *Electromagnetic design sensitivity analysis exploiting the Broyden update*, Master Thesis, Department of Electrical and Computer Engineering, McMaster University.

SMF, Bandler Corporation, P.O. Box 8083, Dundas, ON, Canada L9H 5E7, 2006.

E.A. Soliman, M.H. Bakr and N.K. Nikolova, "Accelerated gradient-based optimization of planar circuits," *IEEE Trans. Antennas Propagat*., vol. 53, Feb. 2005, pp. 880-883.

M. B. Steer, J.W. Bandler and C. M. Snowden, "Computer-aided design of RF and microwave circuits and systems," *IEEE Trans. Microwave Theory Tech*., vol. 50, Mar. 2002, pp. 996-1005.

D.G. Swanson, Jr. and W.J.R. Hoefer, *Microwave Circuit Modeling Using Electromagnetic Filed Simulation*, Artech House, 2003.

F. Tavakkol-Hamedani, L.Shafai and G. Z. Rafi, "The effects of substrate and ground plane size on the performance of finite rectangular microstrip antennas," *IEEE AP-S/URSI Int. Symp. on Antennas Propagat.*, June 2002.

J.P. Webb, "Design sensitivity of frequency response in 3-D finite-element analysis of microwave devices*," IEEE Trans. Magnetics*, vol. 38, Mar. 2002, pp. 1109-1112.

K.-L. Wu, Y.-J. Zhao, J. Wang and M.K.K Cheng, "An effective dynamic coarse model for optimization design of LTCC RF circuits with aggressive space mapping," *IEEE Trans. Microwave Theory Tech*., vol. 52, Jan. 2004, pp. 393-402.

XFDTD, Remcom Inc., 315 South Allen Street, Suite 222, State College, PA 16801, USA.

J. Zhu, "Sensitivity analysis of high-frequency structures with commercial software based on the method of moments," Computational Electromagnetics Res. Lab., McMaster University, CEM-R-23, Jun. 2005.

J. Zhu, "Time comparison and error estimation of the self-adjoint sensitivity analysis of network parameters with the method of moments," Computational Electromagnetics Res. Lab., McMaster University, CEM-R-24, Jun. 2005.

BIBLIOGRAPHY

J. Zhu, J. W. Bandler, N. K. Nikolova and S. Koziel, "Antenna design through space mapping optimization," *IEEE MTT-S Int. Microwave Symp*., San Francisco, California, 2006.

J. Zhu, J.W. Bandler, N.K. Nikolova and S. Koziel, "Antenna optimization through space mapping," submitted to *IEEE Trans. Antennas Propagat., Special Issue on Synthesis and Optimization Techniques in Electromagnetics and Antenna System Design*, Jan. 2007.

J. Zhu, N.K. Nikolova and J. W. Bandler, "Self-adjoint sensitivity analysis of high-frequency structures with FEKO," the *22nd International Review of Progress in Applied Computational Electromagnetics Society* (*ACES 2006*), Miami, Florida, pp. 877-880.

AUTHOR INDEX

A

B

C

D

G

H

I

J

K

L

M

N

P

R

S

T

W

Y

Z

AUTHOR INDEX

SUBJECT INDEX

A

B

C

D

E

F

G

H

I

J

M

O

P

S

T